

ANL-PHY-8758-TH-97  
 hep-ph/9707327

UNITU-THEP-12/1997  
 TU-GK-6/97

## A Solution to Coupled Dyson–Schwinger Equations for Gluons and Ghosts in Landau Gauge

Lorenz von Smekal<sup>a</sup>

Physics Division, Argonne National Laboratory,  
 Argonne, Illinois 60439-4843, USA

Andreas Hauck and Reinhard Alkofer

Institut für Theoretische Physik, Universität Tübingen,  
 Auf der Morgenstelle 14, 72076 Tübingen, Germany

### Abstract

A truncation scheme for the Dyson–Schwinger equations of QCD in Landau gauge is presented which implements the Slavnov–Taylor identities for the 3–point vertex functions. Neglecting contributions from 4–point correlations such as the 4–gluon vertex function and irreducible scattering kernels, a closed system of equations for the propagators is obtained. For the pure gauge theory without quarks this system of equations for the propagators of gluons and ghosts is solved in an approximation which allows for an analytic discussion of its solutions in the infrared: The gluon propagator is shown to vanish for small spacelike momenta whereas the ghost propagator is found to be infrared enhanced. The running coupling of the non–perturbative subtraction scheme approaches an infrared stable fixed point at a critical value of the coupling,  $\alpha_c \simeq 9.5$ . The gluon propagator is shown to have no Lehmann representation. The results for the propagators obtained here compare favorably with recent lattice calculations.

### Keywords

Running coupling constant; Non–perturbative QCD; Gluon propagator; Dyson–Schwinger equations; Infrared behavior; Confinement.

PACS numbers: 02.30.Rz 11.10.Hi 11.15.Tk 12.38.Aw 12.38.Lg 14.70.Dj

---

<sup>a</sup>Address after Nov. 1st, 1997: Institut für Theoretische Physik III, Universität Erlangen–Nürnberg, Staudtstr. 7, 91058 Erlangen, Germany.

# 1 Introduction

The mechanism for confinement of quarks and gluons into colorless hadrons still is little understood. Some theoretical insight could be obtained from disproving the cluster decomposition property for color-nonsinglet gauge-covariant operators. One idea in this direction is based on the possible existence of severe infrared divergences, *i.e.*, divergences which cannot be removed from physical cross sections by a suitable summation over degenerate states by virtue of the Kinoshita–Lee–Nauenberg theorem [1]. Such divergences can provide damping factors for the emission of colored states from color-singlet states (see [2]). However, the Kinoshita–Lee–Nauenberg theorem applies to non-Abelian gauge theories in four dimensions order by order in perturbation theory [3]. Therefore, such a description of confinement in terms of perturbation theory is impossible. In fact, extended to Green’s functions, the absence of unphysical infrared divergences implies that the spectrum of QCD necessarily includes colored quark and gluon states to every order in perturbation theory [4].

An alternative way to understand the insufficiency of perturbation theory to account for confinement in four dimensional field theories is that confinement requires the dynamical generation of a physical mass scale. In presence of such a mass scale, however, the renormalization group [RG] equations imply the existence of essential singularities in physical quantities, such as the  $S$ -matrix, as functions of the coupling at  $g = 0$ . This is because the dependence of the RG invariant confinement scale on the coupling and the renormalization scale  $\mu$  near the ultraviolet fixed point is determined by [5]

$$\Lambda = \mu \exp \left( - \int^g \frac{dg'}{\beta(g')} \right) \xrightarrow{g \rightarrow 0} \mu \exp \left( - \frac{1}{2\beta_0 g^2} \right), \quad \beta_0 > 0. \quad (1)$$

Since all RG invariant masses in massless QCD will exhibit the behavior (1) up to a multiplicative constant the ratios of all bound state masses are, at least in the chiral limit, determined independent of all parameters.

Therefore, to study the infrared behavior of QCD amplitudes non-perturbative methods are required. In addition, as singularities are anticipated, a formulation in the continuum is desirable. One promising approach to non-perturbative phenomena in QCD is provided by studies of truncated systems of its Dyson–Schwinger equations [DSE], the equations of motion for QCD Green’s functions. Typical truncation schemes resort to additional sources of information like the Slavnov–Taylor identities, as entailed by gauge invariance, to express vertex functions and higher  $n$ -point functions in terms of the elementary two-point functions, *i.e.*, the quark, ghost and gluon propagators. In principle, these propagators can then be obtained as selfconsistent solutions to the non-linear integral equations representing the closed set of truncated DSEs.

The underlying conjecture to justify such a truncation of the originally infinite set of DSEs is that a successive inclusion of higher  $n$ -point functions in selfconsistent calculations will not result in dramatic changes to previously obtained lower  $n$ -point

functions. To achieve this it is important to incorporate as much independent information as possible in constructing those  $n$ -point functions which close the system. Such information, *e.g.*, from implications of gauge invariance or symmetry properties, can be relied on being reproduced from solutions to subsequent truncation schemes.

So far, available solutions to truncated Dyson–Schwinger equations of QCD do not even fully include all contributions of the propagators itself. In particular, even in absence of quarks, solutions for the gluon propagator in Landau gauge used to rely on neglecting ghost contributions [6, 7, 8, 9] which, though numerically small in perturbation theory, are unavoidable in this gauge. While this particular problem can be avoided by ghost free gauges such as the axial gauge, in studies of the gluon Dyson–Schwinger equation in the axial gauge [10, 11, 12], the possible occurrence of an independent second term in the tensor structure of the gluon propagator has been disregarded [13]. In fact, if the complete tensor structure of the gluon propagator in axial gauge is taken into account properly, one arrives at a coupled system of equations which is of similar complexity as the ghost–gluon system in the Landau gauge and which is yet to be solved [14].

In addition to providing a better understanding of confinement based on studies of the behavior of QCD Green’s functions in the infrared, DSEs have proven successful in developing a hadron phenomenology which interpolates smoothly between the infrared (non–perturbative) and the ultraviolet (perturbative) regime, for recent reviews see, *e.g.*, [15, 16]. In particular, a dynamical description of the spontaneous breaking of chiral symmetry from studies of the DSE for the quark propagator is well established in a variety of models for the gluonic interactions of quarks [17]. For a sufficiently large low–energy quark–quark interaction quark masses are generated dynamically in the quark DSE in some analogy to the gap equation in superconductivity. This in turn leads naturally to the Goldstone nature of the pion and explains the smallness of its mass as compared to all other hadrons [18]. In this framework a description of the different types of mesons is obtained from Bethe–Salpeter equations for quark–antiquark bound states [19]. Recent progress towards a solution of a fully relativistic three–body equation extends this consistent framework to baryonic bound states [20, 21, 22].

In this paper we present a truncation scheme for the Dyson–Schwinger equations of QCD in Landau gauge which implements the Slavnov–Taylor identities for the 3–point vertex functions. Neglecting contributions from 4–point correlations such as the 4–gluon vertex function and irreducible scattering kernels, this yields a closed set of non–linear integral equations for the propagators of gluons, ghosts and, in an obvious extension, also quarks. We present a solution obtained for the pure gauge theory without quarks in a combination of numerical and analytical methods. The organization of the paper is as follows: The general framework is outlined in section 2. In section 3 we review some earlier results in a scheme proposed by Mandelstam which is most easily introduced by further simplifying the general scheme of the preceeding section, and we comment on available axial gauge studies of the gluon propagator. We concentrate on the coupled system of DSEs for gluons and ghosts from section 4

on, in which we introduce an approximation to reduce this system to a set of one-dimensional non-linear integral equations. This approximation is especially designed to preserve the leading behavior of these propagators in the infrared, and we give an analytic discussion of this behavior. In section 5 we introduce the non-perturbative momentum subtraction scheme and discuss the accordingly extended definition of the corresponding running coupling. The actual details of the renormalization, the definition of the renormalization constants and the renormalized ultraviolet finite equations are given in section 6. An extended analytic discussion of the solutions to the renormalized equations in terms of asymptotic expansions, a necessary prerequisite to a numerical solution, is presented in section 7. The numerical results and their discussion will be the issue of section 8. The non-perturbative result for the running coupling, *i.e.*, the strong coupling as function of the renormalization scale, and the corresponding Callan-Symanzik  $\beta$ -function are given in section 9. We compare our results to recent lattice calculations of the gluon and ghost propagators in section 10, discuss the implications on confinement for gluons in section 11, and we wrap things up with our summary and conclusions in section 12. We wish to point out that one main result, the existence of an infrared stable fixed point at a critical value of the coupling  $\alpha_c \simeq 9.5$ , which could, in principle, be obtained independent of the details of the renormalization as well as the numerical methods and results, is found in our previous publication [23]. This result, meaningless in absence of a complete solution, will be incorporated also here in order to make the present paper self-contained.

## 2 A Truncation Scheme for the Propagators of QCD in Landau Gauge

Besides all elementary two-point functions, *i.e.*, the quark, ghost and gluon propagators, the Dyson-Schwinger equation for the gluon propagator also involves the three- and four-point vertex functions which obey their own Dyson-Schwinger equations. These equations involve successive higher  $n$ -point functions, see figure 1. For simplicity we consider the pure gauge theory and neglect all quark contributions. As for the truncation scheme, the extensions necessary to include quarks in future calculations are straightforward and will be given at the end of this section.

A first step towards a truncation of the gluon equation is to neglect all terms with four-gluon vertices. These are the momentum independent tadpole term, an irrelevant constant which vanishes perturbatively in Landau gauge, and explicit two-loop contributions to the gluon DSE. The latter are subdominant in the ultraviolet, and we can therefore expect solutions to have the correct behavior for asymptotically high momenta without those terms. In the infrared it has been argued that the singularity structure of the two-loop terms does not interfere with the one-loop terms [24]. It therefore seems reasonable to study the non-perturbative behavior of the gluon propagator in the infrared without explicit contributions from four-gluon vertices, *i.e.*, the two-loop diagrams in figure 1. Without quarks the renormalized

$$\begin{aligned}
& \text{wavy line with blob}^{-1} = \text{wavy line}^{-1} - \frac{1}{2} \text{wavy line with blob} - \frac{1}{2} \text{wavy line with blob and circle} \\
& - \frac{1}{6} \text{wavy line with blob and circle} - \frac{1}{2} \text{wavy line with blob and circle} \\
& + \text{wavy line with blob and dashed line} + \text{wavy line with blob and solid line} \\
& \text{dashed line with blob}^{-1} = \text{dashed line}^{-1} - \text{dashed line with blob and circle} \\
& \text{solid line with blob}^{-1} = \text{solid line}^{-1} - \text{solid line with blob and circle}
\end{aligned}$$

Figure 1: Diagrammatic representation of the gluon, ghost and quark Dyson–Schwinger equations of QCD. The wiggly, dashed and solid lines represent the propagation of gluons, ghosts and quarks respectively. A filled blob represents a full propagator and a circle indicates a one–particle irreducible vertex.

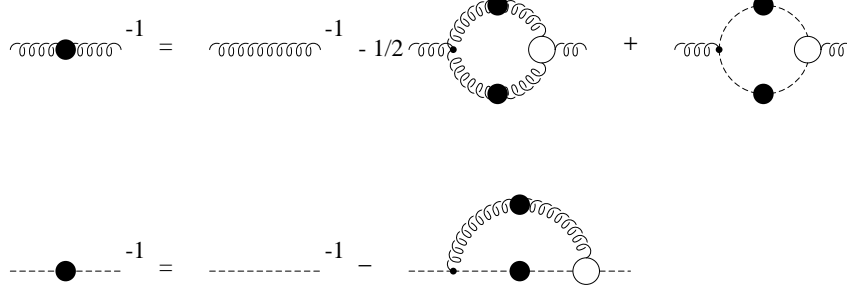


Figure 2: Diagrammatic representation of the gluon and ghost Dyson–Schwinger equations of QCD without quarks. In the gluon DSE terms with four–gluon vertices have been dismissed.

equation for the inverse gluon propagator in Euclidean momentum space with positive definite metric,  $g_{\mu\nu} = \delta_{\mu\nu}$ , (color indices suppressed) is thus given by

$$D_{\mu\nu}^{-1}(k) = Z_3 D_{\mu\nu}^{\text{tl}-1}(k) - g^2 N_c \tilde{Z}_1 \int \frac{d^4 q}{(2\pi)^4} i q_\mu D_G(p) D_G(q) G_\nu(q, p) \quad (2)$$

$$+ g^2 N_c Z_1 \frac{1}{2} \int \frac{d^4 q}{(2\pi)^4} \Gamma_{\mu\rho\alpha}^{\text{tl}}(k, -p, q) D_{\alpha\beta}(q) D_{\rho\sigma}(p) \Gamma_{\beta\sigma\nu}(-q, p, -k) ,$$

where  $p = k + q$ ,  $D^{\text{tl}}$  and  $\Gamma^{\text{tl}}$  are the tree–level propagator and three–gluon vertex,  $D_G$  is the ghost propagator and  $\Gamma$  and  $G$  are the fully dressed 3–point vertex functions. The DSE for the ghost propagator in Landau gauge QCD, without any truncations, will remain unchanged in its form when quarks are included,

$$D_G^{-1}(k) = -\tilde{Z}_3 k^2 + g^2 N_c \tilde{Z}_1 \int \frac{d^4 q}{(2\pi)^4} i k_\mu D_{\mu\nu}(k - q) G_\nu(k, q) D_G(q) . \quad (3)$$

The coupled set of equations for the gluon and ghost propagator, eqs. (2) and (3), is graphically depicted in figure 2. The renormalized propagators for ghosts and gluons,  $D_G$  and  $D_{\mu\nu}$ , and the renormalized coupling  $g$  are defined from the respective bare quantities by introducing multiplicative renormalization constants,

$$\tilde{Z}_3 D_G := D_G^0 , \quad Z_3 D_{\mu\nu} := D_{\mu\nu}^0 , \quad Z_g g := g_0 . \quad (4)$$

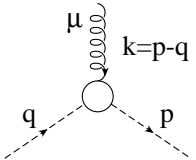
Furthermore,  $Z_1 = Z_g Z_3^{3/2}$ ,  $\tilde{Z}_1 = Z_g Z_3^{1/2} \tilde{Z}_3$ . We use the following notations to separate the structure constants  $f^{abc}$  of the gauge group  $SU(N_c = 3)$  (and the coupling  $g$ ) from the 3–point vertex functions:

$$\Gamma_{\mu\nu\rho}^{abc}(k, p, q) = g f^{abc} (2\pi)^4 \delta^4(k + p + q) \Gamma_{\mu\nu\rho}(k, p, q) . \quad (5)$$

The arguments of the 3-gluon vertex denote the three incoming gluon momenta according to its Lorentz indices (counter clockwise starting from the dot). With this definition, the tree-level vertex has the form,

$$\Gamma_{\mu\nu\rho}^{\text{tl}}(k, p, q) = -i(k-p)_\rho\delta_{\mu\nu} - i(p-q)_\mu\delta_{\nu\rho} - i(q-k)_\nu\delta_{\mu\rho} . \quad (6)$$

The arguments of the ghost-gluon vertex are the outgoing and incoming ghost momenta respectively,

$$G_{\mu}^{abc}(p, q) = gf^{abc}G_{\mu}(p, q) = gf^{abc}iq_{\nu}\tilde{G}_{\mu\nu}(p, q) , \quad (7)$$


where the tensor  $\tilde{G}_{\mu\nu}(p, q)$  contains the ghost-gluon scattering kernel (for its definition see, *e.g.*, ref. [25]). At tree-level this kernel vanishes which corresponds to  $\tilde{G}_{\mu\nu}(p, q) = \delta_{\mu\nu}$ . Note that the color structure of all three loop diagrams in fig. 2 is simply given by  $f^{acd}f^{bdc} = -N_c\delta^{ab}$  which was used in eqs. (2,3) suppressing the trivial color structure of the propagators  $\sim \delta^{ab}$ .

The ghost and gluon propagators in the covariant gauge, introducing the gauge parameter  $\xi$ , are parameterized by their respective renormalization functions  $G$  and  $Z$ ,

$$\begin{aligned} D_G(k) &= -\frac{G(k^2)}{k^2} \quad \text{and} \\ D_{\mu\nu}(k) &= \left(\delta_{\mu\nu} - \frac{k_\mu k_\nu}{k^2}\right) \frac{Z(k^2)}{k^2} + \xi \frac{k_\mu k_\nu}{k^4} . \end{aligned} \quad (8)$$

In order to arrive at a closed set of equations for the functions  $G$  and  $Z$ , we still have to specify a form for the ghost-gluon and the 3-gluon vertex functions. We will now propose a construction of these vertex functions based on Slavnov-Taylor identities as entailed by BRS invariance. For the 3-gluon vertex the general procedure in such a construction was outlined in the literature [25, 26, 27]. Since this procedure involves unknown contributions from the ghost-gluon scattering kernel, it cannot be straightforwardly applied to serve the present purpose, which is to express the vertex functions also in terms of the functions  $G$  and  $Z$ . To this end we have to make additional assumptions on the scattering kernel. Since it is related to the ghost-gluon vertex, we start with the construction of the latter.

For our actual solutions later on, we will be using the Landau gauge ( $\xi = 0$ ) in which one has  $\tilde{Z}_1 = 1$  [28]. Therefore, in the case of the ghost-gluon vertex the choice of its tree-level form in the DSEs may seem justified to the extent that it would at least not affect the leading asymptotic behavior of the solutions in the ultraviolet. This is in contrast to the other vertex functions in QCD which have to be dressed at least in such a way as to account for their anomalous dimensions, if the solutions to

the DSEs in terms of propagators are expected to resemble their leading perturbative behavior at short distances, *i.e.* their correct anomalous dimensions.

A good way to achieve this is to construct vertex functions from their respective Slavnov–Taylor identities. Those identities generally fail, however, to fully constrain the vertex functions. Methods of refinement of such constructions from implications of multiplicative renormalization have been developed for the fermion–photon vertex in QED [29]. Our particular focus in the present context is on the 3–gluon vertex which has a considerably higher symmetry than fermion vertices. This symmetry alleviates the problem of unconstrained terms and we do not expect our results to be overly sensitive to such terms in the 3–gluon vertex.

The Slavnov–Taylor identity for the 3–gluon vertex in momentum space is given by [25, 26, 27],

$$ik_\rho \Gamma_{\mu\nu\rho}(p, q, k) = G(k^2) \left\{ \tilde{G}_{\mu\sigma}(-k, q) \mathcal{P}_{\sigma\nu}(q) \frac{q^2}{Z(q^2)} - \tilde{G}_{\nu\sigma}(-k, p) \mathcal{P}_{\sigma\mu}(p) \frac{p^2}{Z(p^2)} \right\}, \quad (9)$$

where  $\mathcal{P}_{\mu\nu}(k) = \delta_{\mu\nu} - k_\mu k_\nu / k^2$  is the transversal projector. A simple solution to (9) is possible if ghosts are neglected completely, *i.e.*, for  $G(k^2) = 1$  and  $\tilde{G}_{\mu\nu} = \delta_{\mu\nu}$  (see the next section). This is obviously not satisfactory for our present study addressing ghost contributions to the gluon propagator in particular. Given that the anomalous dimension of the ghost–gluon vertex vanishes in Landau gauge, it may seem appealing to retain its tree-level form by setting  $\tilde{G}_{\mu\nu} = \delta_{\mu\nu}$  while taking the presence of the ghost renormalization function  $G(k^2)$  into account in solving (9). Unfortunately, this leads to a contradiction. The Slavnov–Taylor identity for the 3–gluon vertex can be shown to have no solution with this Ansatz. One possibility to resolve this problem is to add a term corresponding to a non-vanishing scattering kernel of the form,

$$\tilde{G}_{\mu\nu}(p, q) = \delta_{\mu\nu} + a(p^2, q^2; k^2) (\delta_{\mu\nu} pq - p_\nu q_\mu). \quad (10)$$

While the additional term in (10) corresponding to a non-trivial ghost–gluon scattering kernel does not contribute to the ghost–gluon vertex (being transverse in  $q_\nu$ ), it is possible to make a minimal Ansatz for the unknown function  $a(x, y; z)$  such that (9) can be solved. The proof that (9) cannot be solved for  $\tilde{G}_{\mu\nu} = \delta_{\mu\nu}$  and the construction of  $a(x, y; z)$  are given in appendix B. This procedure is certainly not unambiguous, and it is furthermore against our original intention to neglect explicit contributions from irreducible four–point functions as it implies a very specific form for the ghost–gluon scattering kernel. A truncation in which the ghost–gluon vertex function is replaced with its tree-level form,  $G_\mu(p, q) \rightarrow iq_\mu$ , while compatible with the desired short distance behavior of the solutions, implies that some non-trivial assumptions on the otherwise unknown ghost–gluon scattering kernel have to be made in order to solve the Slavnov–Taylor identity for the 3–gluon vertex.



In light of this, we prefer a second possibility to resolve the present problem, which is to reconsider the form of the ghost–gluon vertex to start the truncation scheme with. A suitable source of information is provided by a Slavnov–Taylor identity which involves the ghost–gluon vertex directly, similar to the one for the quark–gluon vertex. To our knowledge, such an identity has not been stated in the literature so far. We will therefore outline its derivation from the usual BRS invariance briefly in the following. Neglecting irreducible ghost–ghost scattering, we will arrive at an identity, which allows to express the ghost–gluon vertex in terms of the ghost renormalization function  $G(k^2)$ . The vertex constructed this way will have the correct short distance behavior (no anomalous dimension) and it will constrain  $\tilde{G}_{\mu\nu}(p, q)$  just enough to admit a simple solution to the 3-gluon Slavnov–Taylor identity (9) without further assumptions.

In order to construct a non–perturbatively dressed ghost–gluon vertex, we start from BRS invariance of the generating functional of pure Yang–Mills theory,

$$\delta_{\text{BRS}} Z[\bar{\eta}, \eta, J] = 0 \quad \Leftrightarrow \quad (11)$$

$$\Delta[\bar{\eta}, \eta, J] := \left\langle \int d^4x \left( J^a D^{ab} c^b - \frac{g}{2} f^{abc} \bar{\eta}^a c^b c^c - \frac{1}{\xi} \partial A^a \eta^a \right) \right\rangle_{[\bar{\eta}, \eta, J]} = 0 ,$$

where  $D^{ab} = \delta^{ab} \partial + g f^{abc} A^c$  is the covariant derivative. We retained non–zero sources  $\{\bar{\eta}, \eta, J\}$  for the ghost and gauge fields  $\{c, \bar{c}, A\}$  in order to perform suitable derivatives. Fermion fields have been omitted for simplicity. Their inclusion would not affect the present derivation. We find that the particular derivative of (11) with respect to the sources, suitable to constrain the ghost–gluon vertex, is given by:

$$\frac{\delta^3}{\delta \bar{\eta}^c(z) \delta \eta^b(y) \delta \eta^a(x)} \Delta[\bar{\eta}, \eta, J] \Big|_{\bar{\eta}=\eta=J=0} = 0 , \quad (12)$$

and we obtain

$$\begin{aligned} \frac{1}{\xi} \langle c^c(z) \bar{c}^b(y) \partial A^a(x) \rangle &- \frac{1}{\xi} \langle c^c(z) \bar{c}^a(x) \partial A^b(y) \rangle \\ &= -\frac{g}{2} f^{cde} \langle c^d(z) c^e(z) \bar{c}^a(x) \bar{c}^b(y) \rangle . \end{aligned} \quad (13)$$

Note that this symbolic notation refers to full reducible correlation functions. The two terms on the l.h.s. of (13) can be decomposed in the ghost–gluon proper vertex and the respective propagators. The derivative on the gluon leg thereby projects out the longitudinal part of the gluon propagator which, by virtue of its own Slavnov–Taylor identity  $k_\mu D_{\mu\nu}(k) = \xi k_\nu / k^2$ , remains undressed in the covariant gauge (see eq. (8)). The r.h.s. contains a disconnected part plus terms due to ghost–ghost scattering. At this point we make the truncating assumption mentioned previously. We neglect ghost–ghost scattering contributions to the vertex and retain only the reducible part of the correlation function on the r.h.s. of (13) corresponding to disconnected ghost propagation, *i.e.*,

$$\langle c^c c^a \bar{c}^b \bar{c}^d \rangle = \langle c^a \bar{c}^b \rangle \langle c^c \bar{c}^d \rangle - \langle c^a \bar{c}^d \rangle \langle c^c \bar{c}^b \rangle + \text{connected} . \quad (14)$$

This assumption results in an Abelian Ward–Takahashi type of equation for the ghost–gluon vertex, relating its longitudinal part to a sum of inverse ghost propagators. In momentum space with the ghost renormalization function as introduced in (8) we obtain (for details see appendix A),

$$G(p^2) ik_\rho G_\rho^{abc}(p, q) - G(k^2) ip_\rho G_\rho^{abc}(-k, q) = gf^{abc} \frac{q^2 G(k^2) G(p^2)}{G(q^2)}. \quad (15)$$

Note that this equation is valid for all  $\xi$  including  $\xi = 0$  (Landau gauge). Eq. (15) is solved by the following particularly simple form for the vertex which was also used in ref. [30],

$$G_\mu^{abc}(p, q) = gf^{abc} iq_\mu \frac{G(k^2)}{G(q^2)}. \quad (16)$$

It is important to note, however, that the solution (16) to eq. (15) violates the symmetry properties of the vertex explicitly. In order to check, whether a symmetric solution to (15) exists, we make the general Ansatz,

$$G_\mu(p, q) = i(p + q)_\mu a(k^2; p^2, q^2) - i(p - q)_\mu b(k^2; p^2, q^2). \quad (17)$$

The reason for this particular choice is that in general covariant gauges one has

$$a(x; y, z) = a(x; z, y), \quad (18)$$

whereas the symmetry of  $b(x; y, z)$  is undetermined. In Landau gauge, however, the mixed symmetry term proportional to  $b$  does not contribute to observables directly, since it is purely longitudinal in the gluon momentum. With the Ansatz (17) we find:

$$\begin{aligned} G(x) \left( (z - x) a(y; x, z) + y b(y; x, z) \right) \\ + G(y) \left( (z - y) a(x; y, z) + x b(x; y, z) \right) = \frac{z G(x) G(y)}{G(z)}. \end{aligned} \quad (19)$$

From all terms proportional to  $z$  it follows that

$$a(x; y, z) = \frac{1}{2} \frac{G(x)}{G(z)} + a_1(x, y; z) \frac{1}{G(y)}, \quad a_1(x, y; z) = -a_1(y, x; z).$$

Here the undetermined antisymmetric function  $a_1(x, y; z)$  has to guarantee the symmetry of  $a(x; y, z)$  *c.f.* (18). This can be achieved most easily by setting

$$a_1(x, y; z) = \frac{1}{2} \left( G(x) - G(y) \right) \Rightarrow a(x; y, z) = \frac{1}{2} \left( \frac{G(x)}{G(z)} + \frac{G(x)}{G(y)} - 1 \right).$$

The mixed symmetry term follows readily from terms proportional to  $x$  or  $y$  in (19),

$$b(x; y, z) = \frac{G(x)}{G(y)} a(y; x, z) = \frac{1}{2} \left( \frac{G(x)}{G(z)} - \frac{G(x)}{G(y)} + 1 \right). \quad (20)$$

Collecting the above terms, from (17) the ghost–gluon vertex can be written,

$$G_\mu(p, q) = iq_\mu \frac{G(k^2)}{G(q^2)} + ip_\mu \left( \frac{G(k^2)}{G(p^2)} - 1 \right) \quad (21)$$

$$= iq_\mu \left( \frac{G(k^2)}{G(q^2)} + \frac{G(k^2)}{G(p^2)} - 1 \right) + \text{longitudinal terms} . \quad (22)$$

In the last line we rearranged the terms and displayed explicitly only the ones relevant for the vertex in Landau gauge. While terms longitudinal in the gluon momentum  $k = p - q$  are irrelevant in the vertex, they contribute to the 3–gluon vertex Slavnov–Taylor identity (9). The form of  $\tilde{G}_{\mu\nu}(p, q)$  necessary to generate the complete ghost–gluon vertex (21), is given by

$$\tilde{G}_{\mu\nu}(p, q) = \frac{G(k^2)}{G(q^2)} \delta_{\mu\nu} + \left( \frac{G(k^2)}{G(p^2)} - 1 \right) \frac{p_\mu q_\nu}{q^2} . \quad (23)$$

Here, the last term does not contribute to (9). Therefore, while the relevant term to the ghost–gluon vertex in Landau gauge is given by the one explicitly stated in (22), the term of the tensor (23) to be used in (9) is  $\tilde{G}_{\mu\nu}(p, q) = (G(k^2)/G(q^2)) \delta_{\mu\nu}$  and not what would follow from (22) with the longitudinal terms neglected before constructing  $\tilde{G}$ , *i.e.*,  $(G(k^2)/G(q^2) + G(k^2)/G(p^2) - 1) \delta_{\mu\nu}$ . Additional contributions to  $\tilde{G}_{\mu\nu}(p, q)$  which are purely transverse in  $q_\nu$  can arise from the ghost–gluon scattering kernel. Such terms cannot be constraint from the form of the ghost–gluon vertex. In contrast to the scheme with the tree–level ghost–gluon vertex, where precisely these terms are necessary to solve the 3–gluon Slavnov–Taylor identity, using the dressed vertex (21) and (23), unknown contributions from the ghost–gluon scattering kernel can be neglected in (9). Thus using (23) in (9) we obtain

$$ik_\rho \Gamma_{\mu\nu\rho}(p, q, k) = G(k^2) \left( \mathcal{P}_{\mu\nu}(q) \frac{q^2 G(p^2)}{G(q^2) Z(q^2)} - \mathcal{P}_{\mu\nu}(p) \frac{p^2 G(q^2)}{G(p^2) Z(p^2)} \right), \quad (24)$$

which is only slightly generalized as compared to the *Abelian* like identity obtained neglecting ghosts completely. Using the symmetry of the vertex the solution to (24) fixes the vertex up to completely transverse parts. It can be derived straightforwardly along the lines of the general procedure outlined in [26, 27]. In the present case, the solution is

$$\begin{aligned} \Gamma_{\mu\nu\rho}(p, q, k) = & -A_+(p^2, q^2; k^2) \delta_{\mu\nu} i(p - q)_\rho - A_-(p^2, q^2; k^2) \delta_{\mu\nu} i(p + q)_\rho \\ & - 2 \frac{A_-(p^2, q^2; k^2)}{p^2 - q^2} (\delta_{\mu\nu} p q - p_\nu q_\mu) i(p - q)_\rho + \text{cyclic permutations} , \end{aligned} \quad (25)$$

with

$$A_\pm(p^2, q^2; k^2) = G(k^2) \frac{1}{2} \left( \frac{G(q^2)}{G(p^2) Z(p^2)} \pm \frac{G(p^2)}{G(q^2) Z(q^2)} \right) . \quad (26)$$

At this point, additional unconstrained transverse terms in the vertex are ignored. A counter example for this to be justified is the fermion–photon vertex in QED, for which it has been shown that the transverse part is crucial for multiplicative renormalizability (see, refs. [29]). A similar construction to fix transverse pieces of the vertices in QCD is still lacking. The most important difference, however, which tends to alleviate the problem of undetermined transverse terms in the case of the 3-gluon vertex as constructed from its Slavnov–Taylor identity is its high symmetry. In contrast to the QED fermion vertex, in which 8 of the 12 independent tensor terms are transverse in the photon momentum, in the case of the 3-gluon vertex only 4 out of 14 terms (involving 2 unknown functions) are transverse in all three gluon momenta and thus unconstrained by the Slavnov–Taylor identity (see [26]). Therefore, its Slavnov–Taylor identity together with its full Bose (exchange) symmetry puts much tighter constraints on the 3-gluon vertex than the Ward–Takahashi/Slavnov–Taylor identities do on the fermion–photon/gluon vertices. Note also that there are no undetermined transverse terms in the ghost-gluon vertex of the present truncation scheme.

A further important difference between fermion vertices and the 3-gluon vertex function is that transverse terms in the vertices of (electrons) quarks are of particular importance due to their coupling to transverse (photons) gluons in the Landau gauge. In contrast, for the present purpose of the 3-gluon vertex function, to be used in truncated gluon DSEs, it is well known that the longitudinal contribution to the 3-gluon loop is the one of particular importance [31]. This implies that even though the two gluons within the loop are transverse in Landau gauge, the third (external) leg of the 3-gluon vertex must not be connected to a transverse projector (see below). This makes the important difference, because only the terms that are transverse with respect to all three gluon momenta are unconstrained in the vertex.

Now, we have set up a closed system of equations for the renormalization functions  $G(k^2)$  and  $Z(k^2)$  of ghosts and gluons, consisting of their respective DSEs (2) and (3) with the vertex functions given by (22) and (25/26). Thereby we neglected explicit 4-gluon vertices (in the gluon DSE (2)), irreducible 4-ghost correlations (in the identity for the ghost-gluon vertex (15)) and contributions from the ghost-gluon scattering kernel (to the Slavnov–Taylor identity (9)). This is the most important guideline for our truncation scheme according to the general idea of successively taking higher  $n$ -point functions into account.

It is straightforward to extend the present scheme to selfconsistently include the quark propagator which has the general structure,

$$S(p) = \frac{1}{-i\not{p}A(p^2) + B(p^2)} . \quad (27)$$

For the quark–gluon vertex  $\Gamma_\mu^a(p, q)$  with momentum arguments  $p$  and  $q$  for outgoing and incoming quarks respectively, the Slavnov–Taylor identity is [32],

$$G^{-1}(k^2) i k_\mu \Gamma_\mu^a(p, q) = \left( g t^a - B^a(k, q) \right) i S^{-1}(p) \quad (28)$$

$$-iS^{-1}(q) \left( gt^a - B^a(k, q) \right), \quad k = p - q.$$

Here,  $t^a$  is the  $SU(3)$  generator in the fundamental representation, and  $B^a(k, q)$  is the ghost–quark scattering kernel which again represents irreducible 4–point correlations. In the present truncation scheme in which such 4–point correlations are consistently neglected, the solution to this Slavnov–Taylor identity is obtained from a particularly simple extension to the construction of Ball and Chiu for the solution to the analogous Ward–Takahashi identity of Abelian gauge theory [33]. For  $B^a(k, q) = 0$  the Slavnov–Taylor identity for the quark–gluon vertex (28) is solved by

$$\Gamma_\mu^a(p, q) = -gt^a G(k^2) \left\{ \frac{1}{2} \left( A(p^2) + A(q^2) \right) i\gamma_\mu + \frac{p_\mu + q_\mu}{p^2 - q^2} \left( \left( A(p^2) - A(q^2) \right) \frac{i\not{p} + i\not{q}}{2} - \left( B(p^2) - B(q^2) \right) \right) \right\} + \text{transverse terms} . \quad (29)$$

This is justified for a study with emphasis on the infrared behavior of the propagators even beyond the present truncation scheme, because it has been shown that  $B^a(k, q) \rightarrow 0$  for  $k \rightarrow 0$  in Landau gauge [28]. Note that the only difference to the Abelian case considered in [33] at this point is the presence of the ghost renormalization function appearing in the quark–gluon vertex in Landau gauge. This being a minor modification to the structure of the vertex, the ghost renormalization function in (29) is, however, crucial for the vertex to resemble its correct anomalous dimension in the perturbative limit. Furthermore, our present solution demonstrates that the ghost renormalization function  $G(k^2)$ , being infrared enhanced as we will see below, can give an essential contribution to the effective interaction of quarks as part of the quark–gluon vertex also in the infrared.

With the form (29) for the vertex function in the quark DSE, possibly improved by additional transverse terms as discussed for quenched QED in [29], the present truncation scheme is extended to a closed set of equations for all propagators of Landau gauge QCD as parameterized by the four functions  $Z(k^2)$ ,  $G(k^2)$ ,  $A(k^2)$  and  $B(k^2)$ . Its solution would represent for the first time a systematic and complete solution to the DSEs of QCD at the level of propagators. In the following, we will present our solution to the subset of equations restricted to the pure gauge theory without quarks. The selfconsistent inclusion of the quark DSE will be subject to further investigations.

### 3 The Infrared Behavior of the Gluon Propagator in Previous DSE Studies

Before we turn to the discussion of the coupled system of DSEs for gluons and ghosts and its simultaneous solution in an one–dimensional approximation in the following sections, we briefly review the current status in DSE studies of the gluon propagator

in Landau gauge which is of particular relevance to our present scheme going beyond an approximation by Mandelstam that was previously employed in these studies. For comparison we also summarize available axial gauge studies of the gluon propagator. Their review is necessarily incomplete and we refer the reader to the quoted literature for further information.

A first approximation scheme for the gluon Dyson–Schwinger equation in Landau gauge was originally proposed by Mandelstam [6]. Compared to the scheme outlined above, it consists of a further truncating assumption which is, even though working in Landau gauge, to neglect all ghost contributions to the gluon DSE in pure QCD (without quarks). As a justification for this, it was usually referred to perturbative calculations which yield numerically small ghost contributions to the gluon self-energy. Even though there was never any doubt about the importance of ghosts for fundamental reasons such as transversality of the gluon propagator and unitarity, it was asserted that their quantitative contributions to many hadronic observables might remain negligible even beyond perturbation theory. We will see in the following sections that our present solutions to the coupled system of gluon *and* ghost DSEs, in the systematic truncation scheme outlined above, yield qualitatively quite different results as compared to the Mandelstam approximation, and are thus counter examples to this assertion.

Without ghosts, the solution to the Slavnov–Taylor identity for the 3–gluon vertex is obtained from eq. (24) by setting  $G = 1$ , *i.e.*, eq. (25) with

$$A_{\pm}(p^2, q^2; k^2) = A_{\pm}(p^2, q^2) = \frac{1}{2} \left( \frac{1}{Z(p^2)} \pm \frac{1}{Z(q^2)} \right) . \quad (30)$$

Assuming that  $Z(p^2)$  is a slowly varying function one may then approximate the corresponding solution (25) by

$$\Gamma_{\mu\nu\rho}(p, q, k) = A_+(p^2, q^2) \Gamma_{\mu\nu\rho}^{\text{tl}}(p, q, k) . \quad (31)$$

While this form for the full three–gluon vertex simplifies the 3–gluon loop in the gluon DSE even more than the use of another bare vertex, *i.e.*,  $\Gamma = \Gamma^{\text{tl}}$ , it was observed by Mandelstam to be superior to the latter since it accounts for some of the dressing of the vertex as it results from the corresponding Slavnov–Taylor identity. The nature of this dressing is such that it cancels the dressing of one of the gluon propagators in the 3–gluon loop, and without ghost contributions the gluon DSE (2) in the Mandelstam approximation thus simplifies to

$$\begin{aligned} D_{\mu\nu}^{-1}(k) &= Z_3 D_{\mu\nu}^{\text{tl}-1}(k) \\ &+ g^2 N_c \frac{1}{2} \int \frac{d^4 q}{(2\pi)^4} \Gamma_{\mu\rho\alpha}^{\text{tl}}(k, -p, q) D_{\alpha\beta}(q) D_{\rho\sigma}^{\text{tl}}(p) \Gamma_{\beta\sigma\nu}^{\text{tl}}(-q, p, -k) , \end{aligned} \quad (32)$$

where  $p = k + q$ . This equation, the Mandelstam equation, is schematically depicted in fig. 3. It was already pointed out by Mandelstam that in order to solve this equation selfconsistently it is necessary to implement an additional constraint: Without ghosts

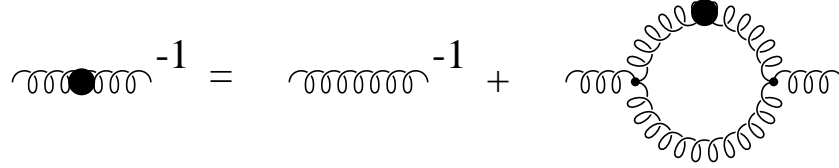


Figure 3: Diagrammatic representation of the gluon Dyson–Schwinger equation in Mandelstam’s approximation.

the Slavnov–Taylor identity (24) with  $G = 1$  and its solution (25/30) for  $p^2 \rightarrow 0$  entail that

$$\lim_{k^2 \rightarrow 0} \frac{k^2}{Z(k^2)} = 0, \quad \text{or} \quad \lim_{k^2 \rightarrow 0} D_{\mu\nu}^{-1}(k^2) = 0 \quad . \quad (33)$$

While imposing this additional condition seems consistent with the other assumptions in the Mandelstam approximation, it has to be emphasized that concluding (33) as a result of (24) relies solely on neglecting all ghost contributions in covariant gauges (see also the discussion at the end of the next section).

The Mandelstam equation in its original form is obtained from eq. (32) upon contraction with the transversal projector  $\mathcal{P}_{\mu\nu}(k) = \delta_{\mu\nu} - k_\mu k_\nu / k^2$  and integration of the angular variables,

$$\begin{aligned} \frac{1}{Z(k^2)} &= Z_3 + \frac{g^2}{16\pi^2} \int_0^{k^2} \frac{dq^2}{k^2} \left( \frac{7}{8} \frac{q^4}{k^4} - \frac{25}{4} \frac{q^2}{k^2} - \frac{9}{2} \right) Z(q^2) \\ &+ \frac{g^2}{16\pi^2} \int_{k^2}^{\Lambda^2} \frac{dq^2}{k^2} \left( \frac{7}{8} \frac{k^4}{q^4} - \frac{25}{4} \frac{k^2}{q^2} - \frac{9}{2} \right) Z(q^2) . \end{aligned} \quad (34)$$

The quadratic ultraviolet divergence in this equation is absorbed by a suitably added counter term introduced in order to account for the masslessness condition (33), see refs. [6, 7]. The solution to this equation proposed by Mandelstam’s infrared analyses proceeds briefly as follows: Assume  $Z(k^2) \sim 1/k^2$ . On the r.h.s of eq. (34) this exclusively yields contributions which violate the masslessness condition (33). Such terms have to be subtracted. Since the kernel on the r.h.s of eq. (34) is linear in  $Z$ , this is achieved by simply subtracting the corresponding contribution from  $Z$  in the integrand. Thus defining

$$Z(k^2) = \frac{b}{k^2} + C(k^2) , \quad b = \text{const.} \quad (35)$$

and retaining only the infrared subleading second term in the integrals, eq. (34) leads to a non–linear integral equation for the function  $C(k^2)$  which, as a solution to this

equation, can be shown to vanish in the infrared by some non-integer exponent of the momentum [6],

$$C(k^2) \sim (k^2)^{\gamma_0}, \quad \gamma_0 = \sqrt{\frac{31}{6}} - 1 \simeq 1.273, \quad \text{for } k^2 \rightarrow 0. \quad (36)$$

Subsequently, an existence proof, a discussion of the singularity structure and an asymptotic expansion of the solution generalizing Mandelstam's discussion of the leading behavior of  $C(k^2)$  in the infrared was given by Atkinson et al. [7].

It was later observed by Brown and Pennington that it is superior for several quite general reasons, to be discussed in more detail in the next section, to contract eq. (32) with the tensor  $\mathcal{R}_{\mu\nu}(k) = \delta_{\mu\nu} - 4k_\mu k_\nu / k^2$ . This led to a somewhat modified equation for the gluon renormalization function, in particular, without quadratically ultraviolet divergent terms [8],

$$\begin{aligned} \frac{1}{Z(k^2)} = & Z_3 + \frac{g^2}{16\pi^2} \int_0^{k^2} \frac{dq^2}{k^2} \left( \frac{7}{2} \frac{q^4}{k^4} - \frac{17}{2} \frac{q^2}{k^2} - \frac{9}{8} \right) Z(q^2) \\ & + \frac{g^2}{16\pi^2} \int_{k^2}^{\Lambda^2} \frac{dq^2}{k^2} \left( \frac{7}{8} \frac{k^4}{q^4} - 7 \frac{k^2}{q^2} \right) Z(q^2). \end{aligned} \quad (37)$$

In a previous publication [9] we demonstrated that the solution to this equation has an infrared behavior quite similar to the solution of Mandelstam's original equation (34). In particular, explicitly separating the leading infrared contribution according to (35) we obtained a unique solution of the form

$$C(k^2) \sim (k^2)^{\gamma_0}, \quad \gamma_0 = \frac{2}{9} \sqrt{229} \cos \left( \frac{1}{3} \arccos \left( -\frac{1099}{229\sqrt{229}} \right) \right) - \frac{13}{9} \simeq 1.271, \quad (38)$$

for  $k^2 \rightarrow 0$ . We solved both equations, eq. (34) as well as eq. (37), using a combination of numerical and analytic methods. In the infrared, we applied the asymptotic expansion technique of ref. [7] and calculated successive terms recursively. The asymptotic expansions obtained this way were then matched to the iterative numerical solution. The results proved independent of the matching point for a sufficiently wide range of values, see [9] for details.

Logarithmic ultraviolet divergences are absorbed in the gluon renormalization constant  $Z_3$  which can be shown to obey the identity  $Z_g Z_3 = 1$  in Mandelstam approximation [9]. This entails that the product of the coupling and the gluon propagator,  $gD_{\mu\nu}(k)$ , does not acquire multiplicative renormalization in this approximation scheme. Using a non-perturbative momentum subtraction scheme corresponding to the renormalization condition

$$Z(k^2 = \mu^2) = 1 \quad (39)$$

for some arbitrary renormalization point  $\mu^2 > 0$ , the resulting equation can in both cases be cast in a renormalization group invariant form determining the renormal-



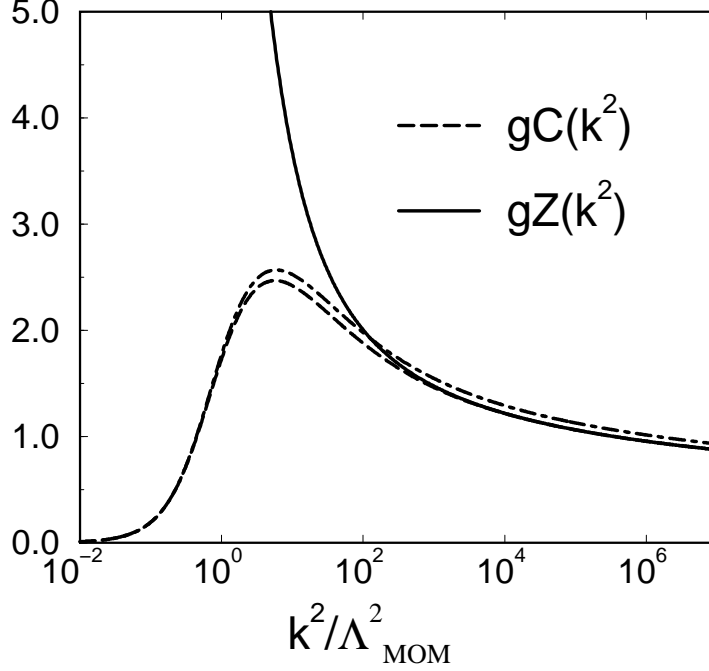


Figure 4: The gluon renormalisation function  $gZ(k^2) = 8\pi\sigma/k^2 + gC(k^2)$  for eq. (37). The dashed lines show the corresponding function  $gC(k^2)$  for eqs. (37) and (34).

ization group invariant product  $gZ(k^2)$  which is equivalent to the running coupling  $\bar{g}(t, g)$  of the scheme,

$$gZ(k^2) = \bar{g}(t_k, g), \quad t_k = \frac{1}{2} \ln k^2/\mu^2. \quad (40)$$

The scaling behavior of the solution near the ultraviolet fixed point is determined by the coefficients  $\beta_0 = 25/2$  and  $\gamma_A^0 = 25/4$  for eq. (34) vs.  $\beta_0 = 14$  and  $\gamma_A^0 = 7$  for (37) which are reasonably close to the perturbative values for  $N_f = 0$ , *i.e.*,  $\beta_0 = 11$  and  $\gamma_A^0 = 13/2$ , the difference being attributed to neglected ghost contributions.

The full non-perturbative solutions to both equations resulting from Mandelstam's approximation scheme, eq. (34) and eq. (37), are compared in figure 4. The most important feature of these results to be noted in the present context is their implication towards an infrared enhanced quark interaction from the (when ghosts are neglected) renormalization group invariant product

$$gD_{\mu\nu}(k) = \mathcal{P}_{\mu\nu}(k) \left( \frac{8\pi\sigma}{k^4} + \frac{gC(k^2)}{k^2} \right) \quad (41)$$

which would allow to identify the string tension  $\sigma$  and relate it to the scale  $\Lambda_{\text{MOM}}$  of the subtraction scheme [9]. The initial question that led to our present study was whether the presence of ghosts in Landau gauge could affect these conclusions.

It is worth mentioning that this result of the Mandelstam approximation, the infrared enhanced gluon propagator (41), was in some contradiction with implications from other studies ranging from lattice calculations [34, 35] to implications from complete gauge fixings [36]. In addition, an alternative approach to studying the Dyson–Schwinger equations of QCD (in Landau gauge) exists which also leads to dissentive conclusions [37, 38]. This approach is based on the observation that an exact vertex function and its perturbative estimate differ by expressions which, in general, contain essential singularities in the coupling of the same structure as in the spontaneous mass scale, see eq. (1). The idea therefore is to improve the perturbative expansion in approximating the Euclidean proper vertices  $\Gamma$  by a double series in the coupling as well as in the degree of a rational approximation with respect to the spontaneous mass scale  $\Lambda_{\text{QCD}}$  being non-analytic in  $g^2$ , *i.e.*, the proper vertices are approximated by a truncated double series in functions  $\Gamma^{(r,l)}$  where  $r$  denotes the degree of the rational approximation while  $l$  represents the loop order of perturbative corrections in  $g^2$  calculated from  $\Gamma^{(r,0)}$  instead of  $\Gamma_{\text{pert.}}^{(0)}$ , see ref. [38]. The requirement that these non-perturbative terms reproduce themselves in the Dyson–Schwinger equations is then used to further restrict the rational Ansätze leaving only a few possible solutions. This method preserves the perturbative renormalizability. However, due to the complexity of the resulting equations the approach has to be restricted to only a few proper vertex functions. These are then taken as a subset of the seven primitively divergent proper vertex functions of QCD: the (inverse) gluon, ghost and quark propagators and the 3-gluon, 4-gluon, gluon-ghost and gluon-quark vertex functions. Preliminary studies within this approach, restricted to  $r = 1$  and  $l = 0$  for pure QCD in Landau gauge and assuming a perturbative ghost propagator, find an infrared vanishing gluon propagator  $\sim k^2$  for small spacelike momenta [37]. A possible problem of this approach might be the existence of light-cone singularities in the 3-gluon vertex function which may be attributed to the low order of the employed approximation. A non-trivial ghost selfenergy becomes unavoidable also in this approach when perturbative corrections are taken into account via Operator Product Expansion techniques [39]. In the meantime several solutions to the order  $r = 1$  and  $l = 1$  have been found. However, even though at the present level the results might not be regarded as absolutely conclusive, neither of these solutions gives rise to an infrared enhancement of the gluon propagator [40].

One might think that the particular problem with ghosts in the Landau gauge can be avoided using gauges such as the axial gauge, in which there are no ghosts in the first place. As for studies of the gluon Dyson–Schwinger equation in the axial gauge [10, 11, 12] it is important to note that, so far, these rely on an assumption on the tensor structure of the gluon propagator. In particular, an independent additional term in the structure of the gluon propagator has not been included in presently available studies of the gluon DSE in axial gauge [13]. This term vanishes in perturbation theory. If, however, the complete tensor structure of the gluon propagator in axial gauge is taken into account properly, one arrives at a coupled system of equations which is of considerably higher complexity than the ghost-gluon system in

the Landau gauge [14]. Some preliminary progress in this direction has so far only been obtained in light-cone gauge [41]. Available studies of the gluon propagator in the axial gauge can therefore not be regarded any more conclusive than those in Landau gauge. In fact, the present situation in axial gauge DSE studies can be summarized to be quite comparable to the Mandelstam approximation in Landau gauge: Early truncation and approximation schemes to the gluon DSE in axial gauge, due to the simplified tensor structure, lead to equations quite similar to Mandelstam's equation [10, 11]. Furthermore, these studies led to an infrared enhanced gluon propagator,  $D(k) \propto \sigma/k^4$  for  $k^2 \rightarrow 0$ , analogous to the solution to Mandelstam's equation [6, 7, 8, 9]. Subsequent studies came to a somewhat dissentive conclusion obtaining an infrared vanishing gluon propagator in the identical scheme in axial gauge [12]. This was, however, later attributed to a sign error in the resulting equation [13]. Therefore, previous DSE studies of the gluon propagator in Landau gauge as well as in the conventional axial gauge seemed to agree in indicating an infrared enhanced gluon propagator  $\propto \sigma/k^4$ . On one hand, such a solution is known to lead to an area law in the Wilson loop [42], on the other hand it was also argued from positivity constraints that the full axial gauge gluon propagator should not be more singular than  $1/k^2$  in the infrared [43]. While this apparent puzzle might be resolved by using suitable principle value prescriptions for the axial gauge singularities [44], it is to be expected that the complete tensor structure of the gluon propagator in the axial gauge will have to be fully taken into account before a more conclusive picture can emerge. As for the Landau gauge, we will find that, instead of the gluon propagator, the previously neglected ghost propagator assumes an infrared enhancement similar to what was then obtained for the gluon.

Progress is desirable in axial gauge as well, of course. A further prerequisite necessary for this, however, will be a proper treatment of the spurious infrared divergences which are well known to be present in axial gauge due to the zero modes of the covariant derivative [44]. This can be achieved by either introducing redundant degrees of freedom, *i.e.* ghosts, also in this gauge [45] (by which it obviously loses its particular advantage) or by using a modified axial gauge [46], which is specially designed to account for those zero modes. Ultimately, progress in more than one gauge will be the only reliable way to assess the influence of spurious gauge dependencies.

## 4 Infrared Dominance of Ghost Contributions

From now on we concentrate on the coupled system of integral equations derived in section 2 for the propagators of gluons *and* ghosts. Instead of attempting its direct numerical solution, we will solve this system simultaneously in an one-dimensional approximation which allows for a thorough analytic discussion of the asymptotic infrared behavior of its solutions. This is necessary in order to obtain stable numerical results from a matching procedure which generalizes the techniques successfully applied to the gluon DSE in Mandelstam approximation [9]. The approximation we use

to arrive at the one-dimensional system of equations is thereby designed to preserve the leading order of the integrands in the infrared limit of integration momenta. At the same time, it will account for the correct short distance behavior of the solutions (behavior at high integration momenta). Because of the particular simplicity of the ghost DSE, we start with this equation to introduce and motivate a modified angle approximation. From (3) with the vertex (22) we obtain the following equation for the ghost renormalization function  $G(k^2)$ ,

$$\begin{aligned} \frac{1}{G(k^2)} &= \tilde{Z}_3 - g^2 N_c \int \frac{d^4 q}{(2\pi)^4} \left( k \mathcal{P}(p) q \right) \frac{Z(p^2) G(q^2)}{k^2 p^2 q^2} \\ &\quad \times \left( \frac{G(p^2)}{G(q^2)} + \frac{G(p^2)}{G(k^2)} - 1 \right), \quad p = k - q. \end{aligned} \quad (42)$$

Here and in the following we use that in Landau gauge  $\tilde{Z}_1 = 1$  [28]. In order to be able to perform the integration over the 4-dimensional angular variables analytically, we make the following approximations:

For  $q^2 < k^2$  we use the angle approximation for the arguments of the functions  $Z$  and  $G$ , *i.e.*,  $G(p^2) = G((k - q)^2) \rightarrow G(k^2)$  and  $Z(p^2) \rightarrow Z(k^2)$ . This obviously preserves the limit  $q^2 \rightarrow 0$  of the integrand.

For  $q^2 > k^2$  we make a slightly different assumption, which is that the functions  $Z$  and  $G$  are slowly varying with their arguments, and we are thus allowed to replace  $G(p^2) \simeq G(k^2) \rightarrow G(q^2)$ . This assumption ensures the correct leading ultraviolet behavior of the equation according to the resummed perturbative result at one-loop level. For all momenta being large, *i.e.* in the perturbative limit, this approximation is well justified by the slow logarithmic momentum dependence of the perturbative renormalization functions for ghosts and gluons. Our solutions will resemble this behavior, justifying the validity of the approximation in this limit.

With this approximation, we obtain from (42) upon angular integration,

$$\begin{aligned} \frac{1}{G(k^2)} &= \tilde{Z}_3 - \frac{g^2}{16\pi^2} \frac{3N_c}{4} \left\{ \int_0^{k^2} \frac{dq^2}{k^2} \frac{q^2}{k^2} Z(k^2) G(k^2) + \int_{k^2}^{\Lambda^2} \frac{dq^2}{q^2} Z(q^2) G(q^2) \right\} \\ &= \tilde{Z}_3 - \frac{g^2}{16\pi^2} \frac{3N_c}{4} \left( \frac{1}{2} Z(k^2) G(k^2) + \int_{k^2}^{\Lambda^2} \frac{dq^2}{q^2} Z(q^2) G(q^2) \right), \end{aligned} \quad (43)$$

where we introduced an  $O(4)$ -invariant momentum cutoff  $\Lambda$  to account for the logarithmic ultraviolet divergence, which will have to be absorbed by the renormalization constant.

A preliminary discussion of the implications of eq. (43) on the infrared behavior of the renormalization functions reveals the following:

Making the Ansatz that for  $x := k^2 \rightarrow 0$  the product of  $G$  and  $Z$  behaves as  $Z(x)G(x) \sim x^\kappa$  for  $\kappa \neq 0$ , it follows readily that

$$G(x) \sim x^{-\kappa} \quad \text{and} \quad Z(x) \sim x^{2\kappa} \quad \text{as} \quad x \rightarrow 0. \quad (44)$$

Furthermore, in order to obtain a positive definite function  $G(x)$  for positive  $x$  from a positive definite  $Z(x)$ , as  $x \rightarrow 0$ , we find the necessary condition  $1/\kappa - 1/2 > 0$  which is equivalent to

$$0 < \kappa < 2. \quad (45)$$

The special case  $\kappa = 0$  leads to a logarithmic singularity in eq. (43) for  $x \rightarrow 0$ . In particular, assuming that  $ZG = c$  with some constant  $c > 0$  and  $x < x_0$  for a sufficiently small  $x_0$ , we obtain  $G^{-1}(x) \rightarrow c(3N_c g^2/64\pi^2) \ln(x/x_0) + \text{const}$  and thus  $G(x) \rightarrow 0^-$  for  $x \rightarrow 0$ , showing that no positive definite solution can be found in this case either.

The gluon DSE (2) is more complicated. In a manifestly gauge invariant formulation the gluon Dyson–Schwinger equation in the covariant gauge would be transverse without further adjustments. For the following decomposition of all its contributions to the inverse gluon propagator:

$$D_{\mu\nu}^{-1}(k) = A(k^2) k^2 \delta_{\mu\nu} - B(k^2) k_\mu k_\nu + \frac{Z_3}{\xi_0} k_\mu k_\nu, \quad (46)$$

this implies that  $A(k^2) = B(k^2) = Z^{-1}(k^2)$ . The longitudinal part of the gluon propagator does not acquire dressing and cancels with the one of the tree-level propagator on the r.h.s. of the gluon DSE (2) ( $\xi = Z_3^{-1} \xi_0$ ). Although we can do our best to use implications of gauge invariance in constructing vertex functions, we cannot expect to arrive at an exactly gauge covariant truncation scheme. This fact is reflected in  $A \neq B$  as obtained from truncated gluon DSEs. An additional source of spurious longitudinal terms in the gluon DSE is the regularization by an  $O(4)$ -invariant Euclidean cutoff  $\Lambda$  which violates the residual local invariance, *i.e.*, the invariance under transformations generated by harmonic gauge functions ( $\partial^2 \Lambda(x) = 0$ ). The straightforward elimination of spurious longitudinal terms by contracting eq. (2) with the transversal projector  $\mathcal{P}_{\mu\nu}(k)$  is known to result in quadratically ultraviolet divergent contributions which are of course artifacts of the regularization not being gauge invariant. As observed by Brown and Pennington [31], in general, quadratic ultraviolet divergences can occur only in  $A(k^2)$ . Therefore, this part cannot be unambiguously determined, it depends on the momentum routing. An unambiguous procedure is to isolate  $B(k^2)$  by contracting the truncated gluon DSE with the projector

$$\mathcal{R}_{\mu\nu}(k) = \delta_{\mu\nu} - 4 \frac{k_\mu k_\nu}{k^2}, \quad (47)$$

and to set  $Z(k^2) = 1/B(k^2)$ . Note that an additional advantage of this prescription is that the constant contribution of the tadpole term in the full gluon DSE does not enter in  $B(k^2)$  either. Since the non-perturbative tadpole does not necessarily vanish, it is in fact an example of a contribution which, if neglected, can lead to  $A \neq B$ . From these various reasons it is clear that one should concentrate on  $B$  rather than  $A$  in truncated gluon DSEs [31, 8].

We gave the detailed justification for this, because it implies that the usual argument of the irrelevance of longitudinal terms in the ghost–gluon vertex in Landau gauge does not apply to the ghost–loop in the gluon DSE (2). We are interested in just the unambiguous term  $B$  proportional to  $k_\mu k_\nu$ . Therefore, contracting (2) with  $\mathcal{R}(k)$ , we see that we have to use the full form of the vertex given in eq. (21) in the gluon DSE. With this and the 3–gluon vertex as given in eqs. (25/26) we obtain,

$$\begin{aligned} \frac{1}{Z(k^2)} &= Z_3 - Z_1 \frac{g^2 N_c}{6} \int \frac{d^4 q}{(2\pi)^4} \left\{ N_1(p^2, q^2; k^2) \frac{Z(p^2)G(p^2)Z(q^2)G(q^2)}{Z(k^2)G^2(k^2)} \right. \\ &\quad + N_2(p^2, q^2; k^2) \frac{Z(p^2)G(p^2)}{G(q^2)} + N_2(q^2, p^2; k^2) \frac{Z(q^2)G(q^2)}{G(p^2)} \left. \right\} \frac{G(k^2)}{k^2 p^2 q^2} \\ &\quad + \frac{g^2 N_c}{3} \int \frac{d^4 q}{(2\pi)^4} \left\{ (q\mathcal{R}(k)q) (G(k^2)G(p^2) - G(q^2)G(p^2)) \right. \\ &\quad \left. - (q\mathcal{R}(k)p) G(k^2)G(q^2) \right\} \frac{1}{k^2 p^2 q^2}. \end{aligned} \quad (48)$$

The functions  $N_1(x, y; z) = N_1(y, x; z)$  and  $N_2(x, y; z)$  are given in appendix C for completeness. These functions have singularities for coinciding arguments canceling only in their sum,  $N_1(x, y; z) + N_2(x, y; z) + N_2(y, x; z)$ , which determines the 3–gluon loop contribution in the Mandelstam approximation [6, 7, 8, 9]. In the present case, the modified angle approximation allows us to combine the three terms of the 3–gluon loop for  $q^2 > k^2$  in the same way as in Mandelstam approximation. For  $q^2 < k^2$ , however, the second term in the 3–gluon loop in (48) can only be combined with the other two by encountering an additional error of the form

$$- Z_1 g^2 \frac{N_c}{6} \int \frac{d^4 q}{(2\pi)^4} N_2(p^2, q^2; k^2) \left( \frac{Z(p^2)G(p^2)}{G(q^2)} - \frac{Z(q^2)G(q^2)}{G(p^2)} \right) \frac{G(k^2)}{k^2 p^2 q^2}. \quad (49)$$

In this contribution the singularity in  $N_2(x, y; z) \sim 1/(x - y)$  is cancelled by the terms in brackets which vanish for  $q^2 \rightarrow p^2$ . However, employing an angle approximation on these terms, the cancellation of the singularity is destroyed and an artificial singular contribution would arise. This demonstrates that approximations have to be used with some care in order to avoid spurious divergences (and imaginary parts). The angle approximation cannot be reasonably applied to the contribution (49). We will omit this contribution to the gluon DSE for  $q^2 < k^2$  in addition to the modified angle approximation, since its inclusion would preclude a one-dimensional reduction of the equations.

Furthermore, this additional approximation has no influence on the motivation for the angle approximation for momenta  $q^2 < k^2$ , *i.e.*, to preserve the infrared limit of the integrands, because all contributions of the 3–gluon loop to the r.h.s in eq. (48) are subleading in the infrared as compared to the contributions of the ghost loop, as our preliminary discussion of the infrared behavior of the solutions reveals (see below). We will therefore put particular emphasis on the ghost contributions to

the coupled system of Dyson–Schwinger equations. In order to isolate their effect, it seems reasonable to treat the 3–gluon loop as analogous as possible to previous studies of the gluon DSE in the Mandelstam approximation. This is achieved by the modified angle approximation to (48), if in addition, for  $q^2 < k^2$ , the contribution (49) in the 3–gluon loop is omitted. This yields from (48) upon angular integration,

$$\begin{aligned} \frac{1}{Z(k^2)} &= Z_3 + Z_1 \frac{g^2}{16\pi^2} \frac{N_c}{3} \left\{ \int_0^{k^2} \frac{dq^2}{k^2} \left( \frac{7}{2} \frac{q^4}{k^4} - \frac{17}{2} \frac{q^2}{k^2} - \frac{9}{8} \right) Z(q^2)G(q^2) \right. \\ &\quad \left. + \int_{k^2}^{\Lambda^2} \frac{dq^2}{q^2} \left( \frac{7}{8} \frac{k^2}{q^2} - 7 \right) Z(q^2)G(q^2) \right\} \\ &\quad + \frac{g^2}{16\pi^2} \frac{N_c}{3} \left\{ \int_0^{k^2} \frac{dq^2}{k^2} \frac{3}{2} \frac{q^2}{k^2} G(k^2)G(q^2) - \frac{1}{3} G^2(k^2) + \frac{1}{2} \int_{k^2}^{\Lambda^2} \frac{dq^2}{q^2} G^2(q^2) \right\}. \end{aligned} \quad (50)$$

The only difference in the 3–gluon loop as obtained here versus the Mandelstam approximation is that the gluon renormalization function  $Z$  is replaced by the product  $ZG$ , see eq. (37) in sec. 3. This is one consequence the presence of the ghost renormalization function has on the dressing of the 3–gluon vertex. The system of equations (43) and (50) is a direct extension to the gluon DSE in the Mandelstam approximation. As such it is very well suited to investigate the influence of ghosts on conclusions of previous studies based on this approximation.

To asses the relative importance of the neglected term (49) we calculated this contribution without angle approximation using, however, the selfconsistent solutions for  $Z(k^2)$  and  $G(k^2)$  as obtained from the one–dimensional set of equations (43) and (50), *c.f.*, the numerical method and results given in section 8 below. In figure 5 we plot the resulting contribution in comparison with the terms retained on the r.h.s. of eq. (50) which, for selfconsistent solutions, are equivalent to  $1/Z(k^2)$ . Though even small terms can, in principle, have a considerable effect on the non–linear selfconsistency problem, the fact that the additional contribution to the gluon DSE due to (49) is comparably small for all momenta supports this additional approximation. In particular, neither the infrared nor the ultraviolet asymptotic regimes are affected by this contribution at all.

Before we turn to the renormalization of equations (43) and (50) in the next sections, we conclude this section with an extension of our preliminary infrared discussion. From (43) we find that  $ZG \rightarrow cx^\kappa$  for  $x \rightarrow 0$  implies,

$$G(x) \rightarrow \left( g^2 \gamma_0^G \left( \frac{1}{\kappa} - \frac{1}{2} \right) \right)^{-1} c^{-1} x^{-\kappa}, \quad \gamma_0^G = \frac{1}{16\pi^2} \frac{3N_c}{4}, \quad (51)$$

$$Z(x) \rightarrow \left( g^2 \gamma_0^G \left( \frac{1}{\kappa} - \frac{1}{2} \right) \right) c^2 x^{2\kappa}, \quad 0 < \kappa < 2, \quad (52)$$

where  $\gamma_0^G$  is the leading order perturbative coefficient of the anomalous dimension of the ghost field. Accordingly, the ghost–loop gives infrared singular contributions  $\sim x^{-2\kappa}$  to the gluon equation (50) while the 3–gluon loop yields terms proportional

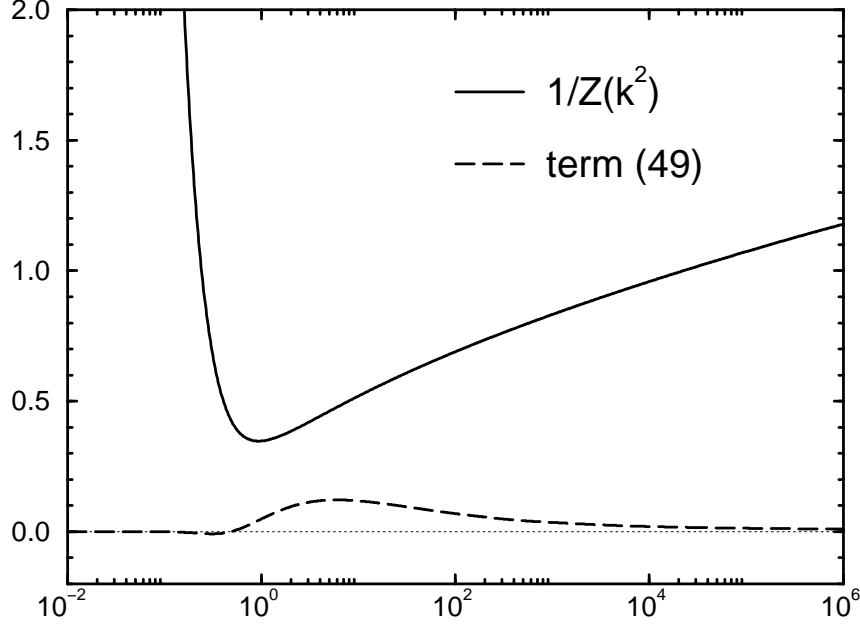


Figure 5: The dismissed contribution (49) (dashed line) compared to the contributions retained on the r.h.s of (50), *i.e.*,  $1/Z(k^2)$  (solid line) as a function of  $x = k^2/\sigma$  with  $\sigma \simeq (350\text{MeV})^2$ , *c.f.*, sec. 8.

to  $x^\kappa$  as  $x \rightarrow 0$ , which are thus subleading contributions to the gluon equation in the infrared. With eq. (51) the leading asymptotic behavior of eq. (50) for  $x \rightarrow 0$  shows that

$$Z(x) \rightarrow g^2 \gamma_0^G \frac{9}{4} \left( \frac{1}{\kappa} - \frac{1}{2} \right)^2 \left( \frac{3}{2} \frac{1}{2-\kappa} - \frac{1}{3} + \frac{1}{4\kappa} \right)^{-1} c^2 x^{2\kappa} \Rightarrow \quad (53)$$

$$\left( \frac{3}{2} \frac{1}{2-\kappa} - \frac{1}{3} + \frac{1}{4\kappa} \right) \stackrel{!}{=} \frac{9}{4} \left( \frac{1}{\kappa} - \frac{1}{2} \right) \Rightarrow \kappa = \frac{61 \stackrel{(+)}{-} \sqrt{1897}}{19} \simeq 0.92. \quad (54)$$

In the last line we compared (53) to (52) and used the restriction (45) obtained from the ghost equation on the exponent  $\kappa$  (ruling out the other sign in (54)). Note that  $\kappa$  is independent of the number of colors  $N_c$ .

This leading behavior of the gluon and ghost renormalization functions and thus their propagators is entirely due to ghost contributions. The details of the treatment of the 3-gluon loop have no influence on above considerations. This is in remarkable contrast to the Mandelstam approximation, in which the 3-gluon loop alone determines the infrared behavior of the gluon propagator and the running coupling in Landau gauge [6, 7, 8, 9]. As a result of this, the running coupling as obtained from the Mandelstam approximation is singular in the infrared [9]. In contrast, as we will show in the next section, the infrared behavior derived from the present truncation



scheme implies an infrared stable fixed point. This is certainly a counter example to the frequently quoted assertion that the presence of ghosts in Landau gauge may have negligible influence on physical observables at hadronic energy scales.

With the infrared behavior of gluon and ghost propagators obtained above, a comment on its implications for the vertex functions is in order. Starting with the ghost–gluon vertex (21) we realize that the limit of vanishing ghost momenta is regular:

$$G_\mu(p, q) \rightarrow -ik_\mu \quad \text{for } p \rightarrow 0 \quad (55)$$

$$G_\mu(p, q) \rightarrow 0 \quad \text{for } q \rightarrow 0 \quad , \quad (56)$$

where we used that  $G(k^2) \sim (k^2)^{-\kappa}$  for  $k^2 \rightarrow 0$ . On the other hand, for vanishing gluon momentum  $k \rightarrow 0$  the vertex diverges as

$$G_\mu(p, q) \rightarrow 2ip_\mu \frac{G(k^2)}{G(p^2)} \sim \frac{2ip_\mu}{G(p^2)} \frac{1}{(k^2)^\kappa} \quad \text{for } k \rightarrow 0 \quad . \quad (57)$$

Since the exponent  $\kappa$  is a (positive) irrational number, see eq. (54), the corresponding divergence cannot be interpreted to reflect the presence of a massless excitation. This divergence is in fact weaker than a massless particle pole ( $\kappa < 1$ ) and presumably lacking a physical interpretation.

Similarly, the 3-gluon vertex as given in equations (25/26) shows analogous infrared divergences resulting from the infrared enhanced ghost renormalization function,

$$\begin{aligned} \Gamma_{\mu\nu\rho}(p, q, k) \rightarrow G(k^2) & \left\{ \left( ip_\mu \delta_{\nu\rho} + ip_\nu \delta_{\mu\rho} - 2ip_\rho \delta_{\mu\nu} \right) \frac{1}{Z(p^2)} \right. \\ & \left. + 2ip_\rho p^2 \mathcal{P}_{\mu\nu}(p) \left( \frac{2G'(p^2)}{G(p^2)Z(p^2)} + \frac{Z'(p^2)}{Z^2(p^2)} \right) \right\} \quad \text{for } k \rightarrow 0 . \end{aligned} \quad (58)$$

This is the correct result to satisfy the differential Slavnov-Taylor identity obtained from eq. (24) for  $k \rightarrow 0$ . Note that in the previous studies of the gluon DSE in Mandelstam approximation [6, 7, 8, 9], the requirement for the 3-gluon vertex function to obey the differential Slavnov–Taylor identity led to the so-called masslessness condition, eq. (33),  $p^2/Z(p^2) \rightarrow 0$  for  $p^2 \rightarrow 0$ . In absence of ghost contributions, the gluon DSE had to be supplemented by this as an additional constraint. This original condition is violated by the infrared behavior of the gluon propagator found here,  $Z(x) \rightarrow x^{2\kappa}$ . The correct replacement of this condition for the present case using (24) with the solution (25/26) is, however,

$$p^2 G(p^2) \rightarrow 0 \quad \text{and} \quad \frac{p^2}{G(p^2)Z(p^2)} \rightarrow 0 \quad \text{for } p^2 \rightarrow 0 . \quad (59)$$

These two necessary conditions are obeyed by the infrared behavior obtained here, *i.e.*,  $G(x) \sim 1/(G(x)Z(x)) \sim x^{-\kappa}$  with  $\kappa \simeq 0.92$  for  $x \rightarrow 0$ , without further adjustments. We see, however, that generally the original bounds on  $\kappa$  obtained from

the consistency of the ghost DSE, when combined with conditions (59), have to be restricted further to  $0 < \kappa < 1$ . The possibility that the masslessness condition in its original form might not hold for non-Abelian gauge theories has been pointed out previously [47, 48]. Our present results support this conjecture.

Finally, since we do not expect quarks to screen the divergence in the ghost renormalization function completely, its presence in the quark-gluon vertex function, see eq. (29), will have a similar effect there, too. We will demonstrate on the example of the running coupling in the next section, how these apparently unphysical divergences in the elementary correlation functions of gluons, ghosts and quarks can, in principle, nevertheless cancel in physical quantities. The lack of a physical interpretation of these divergences (other than maybe reflecting confinement) should, however, not be too surprising for a Euclidean field theory violating reflection positivity (see sec. 11). Note also that in all skeletons of the kernels in relativistic bound state equations for hadrons, the combination of dressed quark-gluon vertices with the non-perturbative gluon propagator will give contributions of the form (*c.f.*, eqs. (28,29)),

$$\sim g^2 G^2(k^2) D_{\mu\nu}(k) \Gamma_\nu^{\text{BC}}(p, p-k) \otimes \Gamma_\mu^{\text{BC}}(q-k, q), \quad (60)$$

where  $\Gamma_\mu^{\text{BC}}(p, q)$  stands for a vertex function with non-perturbative dressing of similar structure to what occurs in an Abelian theory, *e.g.*, a Ball-Chiu construction from its Ward-Takahashi identity. This combination of the ghost renormalization functions with the gluon propagator,  $g^2 G^2(k^2) D(k)$ , in the effective quark interaction is free of the unphysical infrared divergences for  $k \rightarrow 0$ . It is furthermore independent of the renormalization scale in Landau gauge and suited to define a non-perturbative running coupling as we discuss next.

## 5 Subtraction Scheme and Non-Perturbative Running Coupling

Before we discuss the renormalization of the Dyson-Schwinger equations for gluons and ghosts in the next section, some introductory remarks on the choice of the non-perturbative subtraction scheme and its relation to the definition of the running coupling are necessary. In particular, we will see that the preliminary infrared discussion of the last section already yields an important first result: it implies the existence of an infrared fixed point.

We begin with the identity for the renormalization constants (as introduced in eq. (4)),

$$\tilde{Z}_1 = Z_g Z_3^{1/2} \tilde{Z}_3 = 1, \quad (61)$$

which has been shown to hold in the Landau gauge [28]. In fact, our Slavnov-Taylor identity (15) proves that it remains valid in general covariant gauges to the extent that irreducible 4-ghost correlations are neglected. From eq. (61) it follows that the product  $g^2 Z(k^2) G^2(k^2)$  is renormalization group invariant. In absence of any

dimensionful parameter this (dimensionless) product is therefore a function of the running coupling  $\bar{g}$ ,

$$g^2 Z(k^2) G^2(k^2) = f(\bar{g}^2(t_k, g)) , \quad t_k = \frac{1}{2} \ln k^2 / \mu^2 . \quad (62)$$

Here, the running coupling  $\bar{g}(t, g)$  is the solution of  $d/dt \bar{g}(t, g) = \beta(\bar{g})$  with  $\bar{g}(0, g) = g$  and the Callan–Symanzik  $\beta$ -function  $\beta(g) = -\beta_0 g^3 + \mathcal{O}(g^5)$ . The perturbative momentum subtraction scheme is asymptotically defined by  $f(x) \rightarrow x$  for  $x \rightarrow 0$ . This is realized by independently setting

$$Z(\mu^2) = 1 \quad \text{and} \quad G(\mu^2) = 1 \quad (63)$$

for some asymptotically large subtraction point  $k^2 = \mu^2$ . If the invariant product  $g^2 Z(k^2) G^2(k^2)$  is to have a physical meaning, *e.g.*, in terms of a potential between static color sources, it should be independent under changes  $(g, \mu) \rightarrow (g', \mu')$  according to the renormalization group for arbitrary scales  $\mu'$ . Therefore,

$$g^2 Z(\mu'^2) G^2(\mu'^2) \stackrel{!}{=} g'^2 = \bar{g}^2(\ln(\mu'/\mu), g) , \quad (64)$$

and,  $f(x) \equiv x, \forall x$ . We adopt this as a physically sensible definition of a non-perturbative running coupling in the Landau gauge.

This definition is an extension to the one we used in the Mandelstam approximation, eq. (40). In ref. [9] we proved in this approximation without ghosts the identity  $Z_g Z_3 = 1$  implying that  $gZ(k^2)$  is the renormalization group invariant product in this case. The according identification of this product with the running coupling  $gZ(k^2) = \bar{g}(t_k, g)$  is equivalent to the non-perturbative renormalization condition  $Z(\mu^2) = 1, \forall \mu$  in Mandelstam approximation (in which there is no ghost renormalization function).

In the present case, it is not possible to realize  $f(x) \equiv x$  by simply extending the perturbative subtraction scheme (63) to arbitrary values of the scale  $\mu$ , as this would imply a relation between the functions  $Z$  and  $G$  which is inconsistent with the leading infrared behavior of the solutions discussed in the last section. For two independent functions the condition (63) is in general too restrictive to be used for arbitrary subtraction points. Rather, in extending the perturbative subtraction scheme, one is allowed to introduce functions of the coupling such that

$$Z(\mu^2) = f_A(g) \quad \text{and} \quad G(\mu^2) = f_G(g) \quad \text{with} \quad f_G^2 f_A = 1 , \quad (65)$$

and the limits  $f_{A,G} \rightarrow 1, g \rightarrow 0$ . Using this it is straightforward to see that for  $k^2 \neq \mu^2$  one has ( $t_k = (\ln k^2 / \mu^2)/2$ ),

$$\begin{aligned} Z(k^2) &= \exp \left\{ -2 \int_g^{\bar{g}(t_k, g)} dl \frac{\gamma_A(l)}{\beta(l)} \right\} f_A(\bar{g}(t_k, g)) , \\ G(k^2) &= \exp \left\{ -2 \int_g^{\bar{g}(t_k, g)} dl \frac{\gamma_G(l)}{\beta(l)} \right\} f_G(\bar{g}(t_k, g)) . \end{aligned} \quad (66)$$

Here  $\gamma_A(g)$  and  $\gamma_G(g)$  are the anomalous dimensions of gluons and ghosts respectively, and  $\beta(g)$  is the Callan–Symanzik  $\beta$ -function. Eq. (61) corresponds to the following identity for these scaling functions in Landau gauge:

$$2\gamma_G(g) + \gamma_A(g) = -\frac{1}{g}\beta(g). \quad (67)$$

Therefore, we verify that the product  $g^2 Z G^2$  indeed gives the running coupling (*i.e.*, eq. (62) with  $f(x) \equiv x$ ). Perturbatively, at one-loop level eq. (67) is realized separately, *i.e.*,  $\gamma_G(g) = -\delta\beta(g)/g$  and  $\gamma_A(g) = -(1-2\delta)\beta(g)/g$  with  $\delta = 9/44$  for  $N_f = 0$  and arbitrary  $N_c$ . Non-perturbatively we can separate these contributions from the anomalous dimensions by introducing an unknown function  $\epsilon(g)$ ,

$$\gamma_G(g) =: -(\delta + \epsilon(g))\frac{\beta(g)}{g} \Rightarrow \gamma_A(g) = -(1-2\delta-2\epsilon(g))\frac{\beta(g)}{g}. \quad (68)$$

This allows us to rewrite (66) as follows:

$$\begin{aligned} Z(k^2) &= \left(\frac{\bar{g}^2(t_k, g)}{g^2}\right)^{1-2\delta} \exp\left\{-4 \int_g^{\bar{g}(t_k, g)} dl \frac{\epsilon(l)}{l}\right\} f_A(\bar{g}(t_k, g)), \\ G(k^2) &= \left(\frac{\bar{g}^2(t_k, g)}{g^2}\right)^\delta \exp\left\{2 \int_g^{\bar{g}(t_k, g)} dl \frac{\epsilon(l)}{l}\right\} f_G(\bar{g}(t_k, g)). \end{aligned} \quad (69)$$

This is generally possible, also in the presence of quarks, in which case  $\delta = \gamma_0^G/\beta_0 = 9N_c/(44N_c - 8N_f)$  for  $N_f$  flavors in Landau gauge. The above representation of the renormalization functions expresses clearly that regardless of possible contributions from the unknown function  $\epsilon(g)$ , the resulting exponentials cancel in the product  $G^2 Z$ . For a parameterization of the renormalization functions, these exponentials can of course be absorbed by a redefinition of the functions  $f_{A,G}$ . The only effect of such a redefinition is that the originally scale independent functions  $f_{A,G}(\bar{g}(t_k, g))$  will acquire a scale dependence by this, if  $\epsilon \neq 0$ . We therefore use the form (69) to motivate the following parameterization for  $G$  and  $Z$ ,

$$\begin{aligned} Z(k^2) &= \left(\frac{F(x)}{F(s)}\right)^{1-2\delta} R^2(x), \\ G(k^2) &= \left(\frac{F(x)}{F(s)}\right)^\delta \frac{1}{R(x)} \quad \text{with} \quad x := k^2/\sigma \quad \text{and} \quad s := \mu^2/\sigma, \end{aligned} \quad (70)$$

where  $\sigma$  is some currently unfixed (RG invariant) scale parameter. This obviously implements the renormalization condition  $G^2 Z|_{k^2=\mu^2} = 1$  and from the definition of the running coupling (62) we find that  $\bar{g}^2(t_k, g) \sim F(x)$ . We fix the constant of proportionality for later convenience by setting (with  $\beta_0 = 11N_c/(48\pi^2)$  for  $N_f = 0$  quark flavor),

$$\beta_0 \bar{g}^2(t_k, g) = F(x) \quad \text{and} \quad \alpha_S(\mu) = \frac{g^2}{4\pi} = \frac{1}{4\pi\beta_0} F(s), \quad (71)$$

accordingly. As stated above, in general, a non-trivial contribution from  $\epsilon(g)$  will result in the function  $R$  being scale dependent. For the present truncation scheme it will be possible, however, to obtain explicitly scale independent equations to determine the running coupling  $\sim F$  as well as the function  $R$  thus showing that the solutions for the renormalization functions  $G$  and  $Z$  obey one-loop scaling at all scales. In particular, it implies that the products  $g^{2\delta}G$  and  $g^{2(1-2\delta)}Z$  are separately renormalization group invariants in the present scheme (as they are at one-loop level). As for the renormalization scale dependence, the non-perturbative nature of the result is therefore buried entirely in the result for the running coupling.

We are now in a position to discuss the implications of the preliminary results for the infrared behavior of the solutions  $G$  and  $Z$  at the end of the last section without actually solving equations (50,43). From eqs. (51) and (52) we find for  $k^2 \rightarrow 0$ ,

$$g^2 Z(k^2) G^2(k^2) = \bar{g}^2(t_k, g) \xrightarrow{t_k \rightarrow -\infty} \left( \gamma_0^G \left( \frac{1}{\kappa} - \frac{1}{2} \right) \right)^{-1} =: g_c^2. \quad (72)$$

The critical coupling scales with the number of colors as  $g_c^2 \sim 1/N_c$  implying that in our approach  $g_c^2 N_c$  is constant. This agrees with the general considerations of the large  $N_c$ -limit in which  $g^2 N_c$  is kept fixed as  $N_c$  becomes large [49]. For  $N_c = 3$  and with eq. (54) for  $\kappa$  we obtain  $g_c^2 \simeq 119.1$  which corresponds to a critical coupling  $\alpha_c = g_c^2/(4\pi) \simeq 9.48$ . This is a remarkable result in its own, if compared to the running coupling as it was analogously obtained from the Mandelstam approximation [9]. The dynamical inclusion of ghosts changes the infrared singular coupling of the Mandelstam approximation to an infrared finite one implying the existence of an infrared stable fixed point.

## 6 Renormalization

We discuss the actual renormalization of equations (43) and (50) once again beginning with the simpler and thus more evident case of the ghost DSE. To see the effect of the renormalization condition we use the parameterization (70) of the last section in the ghost DSE (43) and set  $k^2 = \mu^2$  ( $\Leftrightarrow x = s$ ) with  $\beta_0 g^2 = F(s)$  and obtain,

$$R(s) = \tilde{Z}_3 - \delta \left( \frac{1}{2} R(s) F(s) + F^\delta(s) \int_s^L \frac{dy}{y} R(y) F^{1-\delta}(y) \right), \quad (73)$$

where  $L := \Lambda^2/\sigma$  is the ultraviolet cutoff and  $\delta = \gamma_0^G/\beta_0$  ( $= 9/44$  for  $N_f = 0$ ). This determines the renormalization constant  $\tilde{Z}_3$  for arbitrary scales  $s$ . We can use (73) to eliminate  $\tilde{Z}_3$  in (43) and obtain analogously for general  $x \neq s$ ,

$$\frac{R(x)}{F^\delta(x)} - \frac{R(s)}{F^\delta(s)} = \quad (74)$$

$$\delta \left( \frac{1}{2} \left( R(s) F^{1-\delta}(s) - R(x) F^{1-\delta}(x) \right) + \int_s^x \frac{dy}{y} R(y) F^{1-\delta}(y) \right).$$

This equation is now ultraviolet as well as infrared finite. Note that the preliminary infrared analyses corresponds to

$$F(x) \rightarrow a := \beta_0 g_c^2 \simeq 8.3 \quad \text{and} \quad R(x) \rightarrow b x^\kappa, \quad x \rightarrow 0, \quad (75)$$

where  $b$  is some currently unfixed constant depending on the choice of the scale parameter  $\sigma$  which we did not specify so far. Equation (74) is valid for all scales  $s$ , in particular, we may let  $s \rightarrow 0$  to obtain,

$$\frac{R(x)}{F^\delta(x)} = \delta \left( \int_0^x \frac{dy}{y} R(y) F^{1-\delta}(y) - \frac{1}{2} R(x) F^{1-\delta}(x) \right). \quad (76)$$

We can use this equation in (73) exchanging  $x \leftrightarrow s$  to write,

$$\tilde{Z}_3 = F^\delta(s) \left( \delta \int_0^L \frac{dy}{y} R(y) F^{1-\delta}(y) \right). \quad (77)$$

If we use this form for  $\tilde{Z}_3$  in (43), we arrive directly at (76) which shows that it remains valid also for non-zero scales  $s$  (we have thus shown that all  $x$ -dependent terms cancel separately from the  $s$ -dependent ones in eq. (74) with the integration range  $(s, x)$  split into  $(0, s)$  and  $(0, x)$ ). It is instructive to replace the integral in (77) by again using eq. (76) now with  $x \leftrightarrow L$ ,

$$\tilde{Z}_3 = \frac{R(L)}{F^\delta(L)} \left( 1 + \frac{\delta}{2} F(L) \right) F^\delta(s) \xrightarrow{L \rightarrow \infty} \frac{F^\delta(s)}{F^\delta(L)} = \left( \frac{g^2}{g_0^2} \right)^\delta, \quad (78)$$

for the perturbative limits of large  $x$ ,  $F(x) \rightarrow 1/\ln x$  and  $R(x) \rightarrow 1$ , showing nicely the scaling limit, in particular, the possible interpretation of the bare coupling as the running coupling at the cutoff scale in the present scheme. Furthermore, the renormalization constant in the scaling limit (large  $L$ ) becomes identical to the multiplicative factor for finite renormalization group transformations of the ghost propagator,  $\tilde{Z}_3(\mu^2, \mu'^2)$  for  $\mu \rightarrow \mu'$ , at the cutoff scale,  $\tilde{Z}_3 = \tilde{Z}_3(\mu^2, L)$ . This detailed study of the scaling behavior of the ghost DSE justifies the use of the improved angle approximation for integration momenta  $q^2 > k^2$  in this case. We now turn to the gluon DSE using the discussion above as a guideline for the anticipated scaling behavior of the gluon equation (50).

The gluon DSE has the additional problem of the presence of the renormalization constant for the 3-gluon vertex  $Z_1$  in the gluon loop. We will address this issue in the following. The first step is to rewrite (50) with (70) and set  $x = s$ ,

$$\begin{aligned} \frac{1}{R^2(s)} &= Z_3 + Z_1 \frac{F^\delta(s)}{11} \left\{ \int_0^s \frac{dy}{s} \left( \frac{7y^2}{2s^2} - \frac{17y}{2s} - \frac{9}{8} + 7\frac{s}{y} \right) R(y) F^{1-\delta}(y) \right. \\ &\quad \left. + s \frac{7}{8} \int_s^\infty \frac{dy}{y^2} R(y) F^{1-\delta}(y) - \frac{7}{\delta} \frac{\tilde{Z}_3}{F^\delta(s)} \right\} + \frac{F^{1-2\delta}(s)}{11} \left\{ \frac{3}{2} \frac{F^\delta(s)}{R(s)} \right. \\ &\quad \left. \times \int_0^s \frac{dy}{s} \frac{y}{s} \frac{F^\delta(y)}{R(y)} - \frac{1}{3} \frac{F^{2\delta}(s)}{R^2(s)} + \frac{1}{2} \int_s^L \frac{dy}{y} \frac{F^{2\delta}(y)}{R^2(y)} \right\}, \end{aligned} \quad (79)$$

where we have used (77) to express the logarithmically divergent term in the 3-gluon loop in terms of the constant  $\tilde{Z}_3$ . Furthermore, we used that the integral  $\int_x^L (dy/y^2) R F^{1-\delta} \rightarrow \int_x^\infty (dy/y^2) R F^{1-\delta}$  is ultraviolet finite for functions  $R$  and  $F$  resembling the perturbative behavior at high momenta. We now have to specify  $Z_1$ . We will discuss three possibilities in the following. The first and probably most obvious will lead to a contradiction. The numerical results of the other two will not show major qualitative differences except at short distances. Comparing to the known perturbative behavior at short distances, we suggest that the third method of treating  $Z_1$  is suited to restore some of the effects of the truncation which are at the root of the present problem.

**a)**  $Z_1 = Z_3/\tilde{Z}_3$

The most rigorous way would be to use the Slavnov–Taylor identity  $Z_1 = Z_3/\tilde{Z}_3$  which follows from  $\tilde{Z}_1 = 1$  in Landau gauge. We could then attempt to eliminate  $Z_3$  from (50) in analogy to (74) for  $x \neq s$  writing,

$$\begin{aligned} \frac{1}{R^2(x)F^{1-2\delta}(x)} - \frac{1}{R^2(s)F^{1-2\delta}(s)} = & \quad (80) \\ & \frac{Z_3 F^\delta(L)}{F^{1-2\delta}(s)} \frac{1}{11} \left\{ \int_0^x \frac{dy}{x} \left( \frac{7}{2} \frac{y^2}{x^2} - \frac{17}{2} \frac{y}{x} - \frac{9}{8} + 7 \frac{x}{y} \right) R(y) F^{1-\delta}(y) \right. \\ & \quad \left. + x \frac{7}{8} \int_x^\infty \frac{dy}{y^2} R(y) F^{1-\delta}(y) - (x \leftrightarrow s) \right\} \\ & + \frac{1}{11} \left\{ \frac{3}{2} \left( \frac{F^\delta(x)}{R(x)} \int_0^x \frac{dy}{x} \frac{y}{x} \frac{F^\delta(y)}{R(y)} - \frac{F^\delta(s)}{R(s)} \int_0^s \frac{dy}{s} \frac{y}{s} \frac{F^\delta(y)}{R(y)} \right) \right. \\ & \quad \left. - \frac{1}{3} \left( \frac{F^{2\delta}(x)}{R^2(x)} - \frac{F^{2\delta}(s)}{R^2(s)} \right) - \frac{1}{2} \int_s^x \frac{dy}{y} \frac{F^{2\delta}(y)}{R^2(y)} \right\}, \end{aligned}$$

where we used  $F^\delta(s)Z_1 = Z_3 F^\delta(L)$  from (78) for large  $L$ . This factor  $Z_3 F^\delta(L)$  is the only cutoff dependence left in (80). Expecting a scaling limit as in the ghost case, *i.e.*,  $Z_3 \rightarrow (F(s)/F(L))^{1-2\delta}$ , we see that the prefactor of the 3-gluon loop contribution to (80) behaves as  $\sim 1/F^{1-3\delta}(L)$  which is singular in the limit  $L \rightarrow \infty$ , if  $1 - 3\delta > 0$ . Perturbatively we expect this to be the case since  $3\delta = 3\gamma_0^G/\beta_0 < 1 \Leftrightarrow \beta_0 > 27/4$  which is true for  $N_f < 7$ . There is no term left in the otherwise ultraviolet finite eq. (80) to absorb the singularity in this case.

It is interesting to note that perturbatively for  $N_f \geq 7$  the leading anomalous dimensions are such that  $Z_1 = Z_3/\tilde{Z}_3 \rightarrow 0$  in the scaling limit in Landau gauge. This implies that the contribution of the 3-gluon loop to the gluon DSE vanishes completely for  $N_f \geq 7$ .

In order to reproduce the leading logarithmic behavior from perturbation theory for high momenta, being determined by  $1 - 3\delta = 17/44$  for  $N_f = 0$ , we find that it is not possible to renormalize the DSEs for gluons and ghosts in the present truncation scheme while retaining the identity  $Z_1 = Z_3/\tilde{Z}_3$ . Could it alternatively be possible to

find a consistent solution for the special case  $1 - 3\delta = 0$ ? Obviously, eq. (80) would have a finite scaling limit in this case. However, a detailed study of the asymptotic behavior of eqs. (76) and (80) shows that this leads to a contradiction. From eq. (76) for large  $x$  with  $R \rightarrow 1$  we obtain a differential equation for  $F$  asymptotically, which has a solution  $F(x) = 1/(\text{const.} + \ln x)$  with  $\delta = 9/(4\beta_0)$ . Therefore, in order to have  $\delta = 1/3$  we need  $\beta_0 = 27/4$ . The same sort of solution is possible asymptotically from (80), however, this time we find  $\delta = 13/(2\beta_0) = 1/3$  which gives the contradiction. The coefficients of the ultraviolet dominant terms of eqs. (76) and (80) are consistent only with the perturbative values for  $\gamma_0^G$ ,  $\gamma_0^A$  and  $\beta_0$ . We therefore conclude that it is necessary to stay with the perturbative short distance character of the equations and abandon the identity  $Z_1 = Z_3/\tilde{Z}_3$  instead. These considerations show that our truncation scheme is unable to obey the implications of gauge invariance exactly which may not be surprising after all. However, we will see in c) below that the hope to obey all Slavnov–Taylor identities for the renormalization constants was only slightly too optimistic.

**b)  $Z_1 = 1$**

The rigorous case above being inconsistent for the present truncation scheme, it may seem natural to try the easiest next, setting  $Z_1 = 1$  since this constant is not necessary to absorb any ultraviolet divergences at the present level anyway. We will see below that  $Z_1 = 1$  is essentially equivalent to setting it to an arbitrary (finite) constant  $c_{Z_1}$ . As in the case of the ghost DSE, we look at the limit of eq. (79) for  $s \rightarrow 0$  in which this equation is singular in contrast to the ghost eq. (77). Using the limits (75) the leading behavior of eq. (79) up to contributions vanishing for  $s \rightarrow 0$  is given by,

$$\begin{aligned} \frac{1}{b^2 s^{2\kappa}} &= Z_3 - c_{Z_1} \frac{28}{9} \tilde{Z}_3 + \frac{a}{11} \left\{ \frac{3}{2} \frac{1}{2 - \kappa} - \frac{1}{3} \right\} \frac{1}{b^2 s^{2\kappa}} \\ &\quad + \frac{a^{1-2\delta}}{22} \int_s^L \frac{dy}{y} \frac{F^{2\delta}(y)}{R^2(y)}. \end{aligned} \quad (81)$$

From the definitions of  $\kappa$  and  $a = \beta_0 g_c^2$ , eqs. (54) and (72), we find

$$\frac{a}{11} \left( \frac{3}{2} \frac{1}{2 - \kappa} - \frac{1}{3} \right) = 1 - \frac{a}{11} \frac{1}{4\kappa} \quad \text{and with} \quad \frac{s^{-2\kappa}}{4\kappa} = \frac{1}{2} \int_s^\infty \frac{dy}{y^{1+2\kappa}},$$

we obtain

$$Z_3 = c_{Z_1} \frac{28}{9} \tilde{Z}_3 - \frac{a^{1-2\delta}}{22} \int_0^L \frac{dy}{y} \left( \frac{F^{2\delta}(y)}{R^2(y)} - \frac{a^{2\delta}}{b^2 y^{2\kappa}} \right). \quad (82)$$

We assumed that  $Z_3 = Z_3(s)$  is finite in the limit  $s \rightarrow 0$  which is necessary from eq. (61), since due to the infrared fixed point  $Z_g$  and  $\tilde{Z}_3$  (see eq. (77)) are infrared finite. Furthermore, the above integral exists only if  $F^{2\delta}/R^2 \rightarrow a^{2\delta}/(b^2 y^{2\kappa}) + \mathcal{O}(y^\tau)$ ,  $\tau > 0$ , which we will verify when we come to discuss the infrared expansion of the solutions



for  $R$  and  $F$ . We are now able to eliminate all ultraviolet divergences from the gluon DSE which can be written as

$$\begin{aligned} \frac{1}{R^2(x)F^{1-2\delta}(x)} &= \frac{c_{Z_1}}{a^{1-3\delta}} \frac{1}{11} \left\{ \int_0^x \frac{dy}{x} \left( \frac{7}{2} \frac{y^2}{x^2} - \frac{17}{2} \frac{y}{x} - \frac{9}{8} + 7 \frac{x}{y} \right) R(y) F^{1-\delta}(y) \right. \\ &\quad \left. + x \frac{7}{8} \int_x^\infty \frac{dy}{y^2} R(y) F^{1-\delta}(y) \right\} + \frac{1}{11} \left\{ \frac{3}{2} \frac{F^\delta(x)}{R(x)} \int_0^x \frac{dy}{x} \frac{y}{x} \frac{F^\delta(y)}{R(y)} \right. \\ &\quad \left. - \frac{1}{3} \frac{F^{2\delta}(x)}{R^2(x)} - \frac{1}{2} \int_0^x \frac{dy}{y} \left( \frac{F^{2\delta}(y)}{R^2(y)} - \frac{a^{2\delta}}{b^2 y^{2\kappa}} \right) + \frac{1}{4\kappa} \frac{a^{2\delta}}{b^2 x^{2\kappa}} \right\} . \end{aligned} \quad (83)$$

We see from this equation that with a redefinition  $R' := c_{Z_1}^{1/3} R$  and accordingly  $b' = c_{Z_1}^{1/3} b$  we can eliminate the finite constant  $c_{Z_1}$  from (83). The ghost DSE (76) is linear in  $R$  and thus in its form unchanged by this redefinition. It implies a scaling of the propagators by a multiplicative constant which does not appear in physical quantities like the running coupling and is thus unessential. We will therefore solve the coupled system (76) and (83) for  $Z_1 = c_{Z_1} = 1$ . It is easy to see from those terms in eq. (83) which are dominant for large  $x$ , that the resulting gluon propagator cannot be expected to have the correct perturbative ultraviolet behavior (its perturbative anomalous dimension): The leading ultraviolet contribution from the ghost loop has the wrong sign and should be compensated by the according contribution from the 3-gluon loop. However, in eq. (83) the latter gives a contribution qualitatively equal to the asymptotic behavior of the ghost DSE (76) which is logarithmically subleading as compared to the ghost loop (since  $\tilde{Z}_3/Z_3 \rightarrow 0$  for  $N_f < 7$ ). It is clear that we cannot expect the solutions to resemble the perturbative behavior at asymptotically high momenta for this reason.

Evidently, the insufficiencies of the truncation scheme appear here in the approximations used to simplify the 3-gluon loop. We reiterate, however, that the 3-gluon loop does not affect the leading behavior of the ghost-gluon DSEs in the infrared. We suggest a further manipulation in the following which is motivated by the desired short distance behavior of the solutions and which is suited for its restoration. We will compare our numerical results obtained for  $Z_1 = 1$  to those from the procedure outlined in the following. In particular, this will verify that the additional manipulation improves the short distance (high momentum) behavior of the solutions, and that this is indeed all it does (not affecting conclusions on the infrared behavior).

$$\text{c) } Z_1 = (F(s)/F(y))^{1-3\delta}$$

As a first remark, we note that we found  $\tilde{Z}_3 = (F(s)/F(L))^\delta$  in the scaling limit. Analogously, we would like to obtain  $Z_3 = (F(s)/F(L))^{1-2\delta}$  and  $Z_1 = (F(s)/F(L))^{1-3\delta}$  from the corresponding Slavnov-Taylor identity. We saw above that the latter, *i.e.*,  $Z_1 = Z_3/\tilde{Z}_3$ , was not consistently possible at the present level of truncations. Therefore, we suggest to set  $Z_1 = (F(s)/F(y))^{1-3\delta}$  instead, where  $y = q^2/\sigma$  denotes the loop momentum. We repeat the same steps as before to elimi-

nate the renormalization constants and, in place of eq. (80), we arrive at

$$\begin{aligned} \frac{1}{R^2(x)F^{1-2\delta}(x)} - \frac{1}{R^2(s)F^{1-2\delta}(s)} = & \quad (84) \\ \frac{1}{11} \left\{ \int_0^x \frac{dy}{x} \left( \frac{7}{2} \frac{y^2}{x^2} - \frac{17}{2} \frac{y}{x} - \frac{9}{8} + 7 \frac{x}{y} \right) R(y) F^{2\delta}(y) + x \frac{7}{8} \int_x^\infty \frac{dy}{y^2} R(y) F^{2\delta}(y) \right. \\ & \left. - (x \leftrightarrow s) \right\} + \text{ghost loop contributions} , \end{aligned}$$

where we did not explicitly repeat the unchanged contributions from the ghost loop again (see eq. (80)). If we now repeat the exact same steps as in the case of the ghost DSE, the limit  $s \rightarrow 0$  now leads to

$$\begin{aligned} \frac{11}{R^2(x)F^{1-2\delta}(x)} = & \int_0^x \frac{dy}{x} \left( \frac{7}{2} \frac{y^2}{x^2} - \frac{17}{2} \frac{y}{x} - \frac{9}{8} + 7 \frac{x}{y} \right) R(y) F^{2\delta}(y) \\ & + x \frac{7}{8} \int_x^\infty \frac{dy}{y^2} R(y) F^{2\delta}(y) + \frac{3}{2} \frac{F^\delta(x)}{R(x)} \int_0^x \frac{dy}{x} \frac{y}{x} \frac{F^\delta(y)}{R(y)} - \frac{1}{3} \frac{F^{2\delta}(x)}{R^2(x)} \\ & - \frac{1}{2} \int_0^x \frac{dy}{y} \left( \frac{F^{2\delta}(y)}{R^2(y)} - \frac{a^{2\delta}}{b^2 y^{2\kappa}} \right) + \frac{1}{4\kappa} \frac{a^{2\delta}}{b^2 x^{2\kappa}} , \end{aligned} \quad (85)$$

which can again be use to obtain the gluon renormalization constant, exchanging variables  $x \leftrightarrow s$ , with the result,

$$Z_3 = F^{1-\delta}(s) \left( \frac{7}{11} \int_0^L \frac{dy}{y} R(y) F^{2\delta}(y) - \frac{1}{22} \int_0^L \frac{dy}{y} \left( \frac{F^{2\delta}(y)}{R^2(y)} - \frac{a^{2\delta}}{b^2 y^{2\kappa}} \right) \right). \quad (86)$$

This is analogous to eq. (78) and valid for all  $s$ . Using eq. (85) with  $x \leftrightarrow L$  for large  $L$  we furthermore obtain the desired scaling limit,

$$Z_3 \xrightarrow{L \rightarrow \infty} \left( \frac{F(s)}{F(L)} \right)^{1-2\delta} = \left( \frac{g^2}{g_0^2} \right)^{1-2\delta}. \quad (87)$$

While  $Z_1 = (F(s)/F(y))^{1-3\delta}$  violates the Slavnov–Taylor identity which instead would demand  $Z_1 = (F(s)/F(L))^{1-3\delta}$ , it thus reproduces the correct scaling limit for the gluon propagator. This will be reflected in the numerical solutions, in particular, in the leading logarithmic behavior of the gluon propagator.

Note that eqs. (83) and (85) are equivalent to order  $g^2$  in perturbation theory. One-loop scaling requires, however, that a certain class of diagrams of the perturbative series is subsummed, which includes contributions of orders  $g^4$  and higher. It should therefore not be surprising that a truncation scheme neglecting 4-gluon correlations (which appear at order  $g^4$ ) does not automatically reproduce the perturbative anomalous dimensions. We have seen that this problem is also related to some violation of the implications of gauge invariance.

We will proceed mainly with discussing the solutions to (76) and (85) analytically as well as the numerical results, and use the alternative version (83) only for comparison and in order to demonstrate that our main conclusions such as the existence of the infrared fixed point do not depend on the particular choice for  $Z_1$  in the 3-gluon loop. We will verify that the sole effect of this choice is to fix the behavior of the solutions, in particular, the gluon propagator, at short distances where their anticipated asymptotic perturbative form was used as the guiding principle.

## 7 Asymptotic Expansion and Scale Invariance

The set of equations (76) and (85) does not depend on the scale  $s$  showing that its solutions represent gluon and ghost renormalization functions obeying one-loop scaling at all scales, *i.e.*,  $\epsilon(g) = 0$ , see eqs. (69) and (70). We have thus rewritten the problem in terms of the renormalization group invariant functions  $F(x)$  and  $R(x)$ . In particular, the scaling behavior of the propagators follows trivially from the solution for the non-perturbative running coupling  $F/\beta_0$ .

Similar to our previous solution to the gluon DSE in Mandelstam approximation, a detailed analyses of the solutions in the infrared in terms of asymptotic series is necessary in order to obtain numerically stable iterative solutions. Due to the nature of the coupled set of equations a recursive calculation of the respective coefficients of the asymptotic series for  $F$  and  $R$  is considerably more difficult than in Mandelstam approximation in which simple recursion relations allowed to calculate these coefficients to any desired order [7, 9]. Fortunately, calculating the leading corrections to the asymptotic infrared behavior of  $R$  and  $F$ , as given above, proved sufficient to obtain numerically stable results. Thereby, for  $x < x_0$  with some infrared matching point  $x_0$ , the asymptotic series to at least second order, in a sense to be explained below, is used in obtaining iterative solutions for  $x > x_0$ . The matching point  $x_0$  has to be sufficiently small for the asymptotic series to provide the desired accuracy. However, limited by numerical stability, it cannot be chosen arbitrarily small either. This leads to a certain range of values of  $x_0$  for which stable solutions are obtained with no matching point dependence to fixed accuracy. We verified that the additional inclusion of third order contributions in the asymptotic series has no effect other than increasing the allowed range for the matching point.

The discussion of the solutions in the infrared is alleviated by the observation that one of the equations, eq. (76),

$$\frac{R(x)}{F^\delta(x)} = \delta \left( \int_0^x \frac{dy}{y} R(y) F^{1-\delta}(y) - \frac{1}{2} R(x) F^{1-\delta}(x) \right), \quad (88)$$

can be converted in a first order homogeneous linear differential equation for  $R(x)$ . Differentiating eq. (88) with respect to  $x$  one obtains,

$$R'(x) = T(x)R(x), \quad T(x) := \frac{\delta}{1 + \frac{\delta}{2}F} \left( \frac{F}{x} + \frac{F'}{F} - \frac{1-\delta}{2}F' \right). \quad (89)$$

The second equation to solve, eq. (85), can be written,

$$\begin{aligned} \frac{11}{R^2(x)F^{1-2\delta}(x)} &= \int_0^x \frac{dy}{x} \left\{ \left( \frac{7}{2} \frac{y^2}{x^2} - \frac{17}{2} \frac{y}{x} - \frac{9}{8} + 7 \frac{x}{y} - \frac{7}{8} \frac{x^2}{y^2} \right) R(y) F^{2\delta}(y) \right. \\ &\quad \left. + \frac{7}{8} \frac{x^2}{y^2} b a^{2\delta} y^\kappa \right\} + \frac{7}{8} \frac{b a^{2\delta}}{1-\kappa} x^\kappa + A x + \frac{3}{2} \frac{F^\delta(x)}{R(x)} \int_0^x \frac{dy}{x} \frac{y}{x} \frac{F^\delta(y)}{R(y)} \\ &\quad - \frac{1}{3} \frac{F^{2\delta}(x)}{R^2(x)} - \frac{1}{2} \int_0^x \frac{dy}{y} \left( \frac{F^{2\delta}(y)}{R^2(y)} - \frac{a^{2\delta}}{b^2 y^{2\kappa}} \right) + \frac{1}{4\kappa} \frac{a^{2\delta}}{b^2 x^{2\kappa}}, \end{aligned} \quad (90)$$

where we have used that

$$\begin{aligned} x \frac{7}{8} \int_x^\infty \frac{dy}{y^2} R(y) F^{2\delta}(y) &= -x \frac{7}{8} \int_0^x \frac{dy}{y^2} (R F^{2\delta} - b a^{2\delta} y^\kappa) + \frac{7}{8} \frac{b a^{2\delta}}{1-\kappa} x^\kappa + A x \\ \text{with} \quad A &= \frac{7}{8} \int_0^\infty \frac{dy}{y^2} (R F^{2\delta} - b a^{2\delta} y^\kappa). \end{aligned} \quad (91)$$

From the leading infrared behavior, *i.e.*,  $F \rightarrow a$  and  $R \rightarrow b x^\kappa$  for  $x \rightarrow 0$ , we see from eq. (88) that an asymptotic infrared expansion of  $1/(R^2 F^{1-2\delta})$  has to contain powers of  $x^\kappa$  as well as powers of  $x$  in subsequent subleading terms. This motivates the following Ansatz,

$$R(x) = b x^\kappa \sum_{l,m,n=0}^{\Sigma=N} C_{lmn} x^{m\nu+3n\kappa+l(1+2\kappa)} \quad (92)$$

$$F(x) = a \sum_{l,m,n=0}^{\Sigma=N} D_{lmn} x^{m\nu+3n\kappa+l(1+2\kappa)}, \quad \text{with} \quad \Sigma := l + m + n \quad (93)$$

and  $C_{000} = D_{000} = 1$ . The additional fractional power  $x^\nu$  in these expansions was introduced to find the most important subleading behavior possible from the consistency in the infrared. We will determine it to be  $\nu \simeq 2.05$ . With  $2 < 3\kappa < 1 + 2\kappa \lesssim 3$  this shows that for not too large orders  $N$  powers of different orders in this expansions do not mix in their successive importance at small  $x$ . Furthermore, we have repeatedly subtracted leading infrared contributions explicitly from integrals such as the one in (82) above, assuming that the remaining contributions are integrable for  $x \rightarrow 0$ . For subleading contributions to  $R$  and  $F$  suppressed by powers of  $x^\nu$  with  $\nu \simeq 2.05$  this is justified *a posteriori*.

With the series (93) we can calculate  $T(x)$  in eq. (88) to the same order  $N$ ,

$$T(x) = \frac{\kappa}{x} \sum_{l,m,n=0}^{\Sigma=N} E_{lmn} x^{\tau_{lmn}}, \quad \text{with} \quad \tau_{lmn} := m\nu + 3n\kappa + l(1 + 2\kappa), \quad (94)$$

where the coefficients  $E_{lmn}$  can be straightforwardly calculated from the coefficients  $D_{lmn}$  of  $F$  (with  $E_{000} = 1$ ). The solution of eq. (88) for  $R$  with the integration constant set to  $b$  is then given by

$$R(x) = b x^\kappa \exp \left\{ \kappa \sum_{\Sigma=1}^N \frac{E_{lmn}}{\tau_{lmn}} x^{\tau_{lmn}} \right\}. \quad (95)$$

Expanding this series to an appropriate order allows to relate the coefficients  $C_{lmn}$  to  $E_{lmn}$  and thus to  $D_{lmn}$ . For  $N = 1$  the result is,

$$\begin{aligned} C_{100} &= \frac{\kappa}{1+2\kappa} E_{100} = \left( \frac{\kappa(1-3\kappa)}{2(1+2\kappa)} + \delta \right) D_{100} \\ C_{010} &= \frac{\kappa}{\nu} E_{010} = \left( \frac{\kappa}{\nu} - \frac{\kappa}{2} - \frac{\kappa^2}{2\nu} + \delta \right) D_{010} \\ C_{001} &= \frac{1}{3} E_{001} = \left( \frac{1}{3} - \frac{2}{3}\kappa + \delta \right) D_{001}. \end{aligned} \quad (96)$$

At higher orders in  $N$  this procedure recursively yields relations that uniquely determine the coefficients  $C$  in terms of the coefficients  $D$ . Analogous relations are obtained from eq. (90) by expanding all ratios of  $R$  and  $F$  which occur with dependence on  $x$  and  $y$ , and by comparison of the respective orders,  $\mathcal{O}(x^{\tau_{lmn}-2\kappa})$ , on both sides. We verify from eq. (90) that to leading order,  $\mathcal{O}(x^{-2\kappa})$ :

$$\frac{11}{b^2 a^{1-2\delta}} = \left( \frac{3}{2} \frac{1}{2-\kappa} - \frac{1}{3} + \frac{1}{4\kappa} \right) \frac{a^{2\delta}}{b^2}, \quad (97)$$

which was used to determine  $\kappa$  with  $a = \beta_0 g_c^2 = ((9/44)(1/\kappa - 1/2))^{-1}$  (see eqs. (72) and (54)). At order  $N = 1$  we obtain,

$$\begin{aligned} \mathcal{O}(x^{\nu-2\kappa}) : \quad & \frac{11}{a} (D_{010} + 2(C_{010} - \delta D_{010})) = \\ & \left( \frac{3}{2} \left( \frac{1}{2+\nu-\kappa} + \frac{1}{2-\kappa} \right) - \frac{2}{3} - \frac{1}{\nu-2\kappa} \right) (C_{010} - \delta D_{010}) \end{aligned} \quad (98)$$

$$\begin{aligned} \mathcal{O}(x^\kappa) : \quad & \frac{11}{a} (D_{001} + 2(C_{001} - \delta D_{001})) = -b^3 f(\kappa) + \\ & \left( \frac{3}{2} \left( \frac{1}{2+2\kappa} + \frac{1}{2-\kappa} \right) - \frac{2}{3} - \frac{1}{\kappa} \right) (C_{001} - \delta D_{001}) \end{aligned} \quad (99)$$

$$\begin{aligned} \mathcal{O}(x) : \quad & \frac{11}{a} (D_{100} + 2(C_{100} - \delta D_{100})) = -\frac{b^2}{a^{2\delta}} A + \\ & \left( \frac{3}{2} \left( \frac{1}{3+\kappa} + \frac{1}{2-\kappa} \right) - \frac{5}{3} \right) (C_{100} - \delta D_{100}), \end{aligned} \quad (100)$$

with  $f(\kappa) := 7/(2(3+\kappa)) - 17/(2(2+\kappa)) - 9/(8(1+\kappa)) + 7/\kappa + 7/(8(1-\kappa))$ .

These equations together with eqs. (96) determine the coefficients  $D$  and  $C$  to lowest non-trivial order. In particular, we have 3 decoupled sets of 2 equations each for 2 of the constants, respectively. For  $(l, m, n) = (1, 0, 0)$ , *c.f.*, eq. (100), we obtain,

$$C_{100} \simeq 0.05554 b^2 A, \quad \text{and} \quad D_{100} \simeq -0.6992 b^2 A. \quad (101)$$

The set of equations for  $(l, m, n) = (0, 1, 0)$  is homogeneous, see eq. (98). The determinant of its 2-dimensional coefficient matrix is zero for

$$\nu = \frac{-6 - \kappa - 3\kappa^2 \pm \sqrt{-4(-26 - 23\kappa)\kappa^2(3+2\kappa) + (6 + \kappa + 3\kappa^2)^2}}{2(3+2\kappa)}, \quad (102)$$

with one positive root for the plus sign which determines the positive exponent  $\nu$ . The coefficients  $C_{010}$ ,  $D_{010}$  follow up to a common factor. With  $\kappa = (61 - \sqrt{1897})/19$  we obtain,

$$\nu \simeq 2.051 \quad \text{and} \quad C_{010} = -0.0124 D_{010} . \quad (103)$$

For  $(l, m, n) = (0, 0, 1)$  the scale of the coefficients is set by the inhomogeneity,  $b^3 f(\kappa)$ , in eq. (99) and we obtain,

$$C_{001} \simeq 1.969 b^3 , \quad \text{and} \quad D_{001} \simeq -26.52 b^3 . \quad (104)$$

Using these results, higher orders, though increasingly tedious, can be obtained recursively by analogous sets of equations. The general pattern is such that the order  $N = 1$  above fixes the scales for higher order coefficients. This allows us to define scale independent coefficients  $\tilde{C}$  and  $\tilde{D}$  by extracting their respective scales according to the exponent  $\tau_{lmn} = m\nu + 3n\kappa + l(1 + 2\kappa)$  of  $x$  for a given set  $(l, m, n)$ ,

$$C_{lmn} =: \tilde{C}_{lmn} b^{3n+2l} t^m A^l , \quad \text{and} \quad D_{lmn} =: \tilde{D}_{lmn} b^{3n+2l} t^m A^l , \quad (105)$$

where the scale of the powers of  $x^\nu$  is set by  $t$  which we fix for convenience to

$$t := -D_{010} \quad (106)$$

*i.e.*,  $\tilde{C}_{010} \simeq 0.0124$  and  $\tilde{D}_{010} = -1$ . We summarize the values of the coefficients  $\tilde{C}$  and  $\tilde{D}$  for  $N = 2$  in table 1.

$(l, m, n)$	$(2, 0, 0)$	$(1, 1, 0)$	$(1, 0, 1)$	$(0, 2, 0)$	$(0, 1, 1)$	$(0, 0, 2)$
$\tilde{C}$	-0.1042	-0.3034	-7.933	-0.2160	-11.55	-151.0
$\tilde{D}$	0.5246	1.590	40.10	1.226	60.98	766.8

Table 1: Coefficients of the asymptotic expansion for  $N = 2$ .

The constant  $A$  as given in (91) is determined numerically in the iterative process. Of the remaining two parameters  $b$  and  $t$  in the asymptotic forms, one can be related to the overall momentum scale so that we are left with one independent parameter. Note that we neither specified the momentum scale  $\sigma$  (in  $x = k^2/\sigma$ ) nor the infrared constant  $b$  so far. The problem is scale invariant, however, *i.e.*, a change in the scale  $\sigma$  according to  $\sigma \rightarrow \sigma' = \sigma/\lambda$  or, equivalently,  $x \rightarrow x' = \lambda x$  can be compensated by

$$b \rightarrow b' = b/\lambda^\kappa , \quad \text{and} \quad t \rightarrow t' = t/\lambda^\nu . \quad (107)$$

We can thus choose the scale without loss of generality such that the positive number  $b = 1$ . The parameter  $t$  can in principle be any real number including zero. We can find numerically stable iterative solutions for not too large absolute values of  $t$  (see

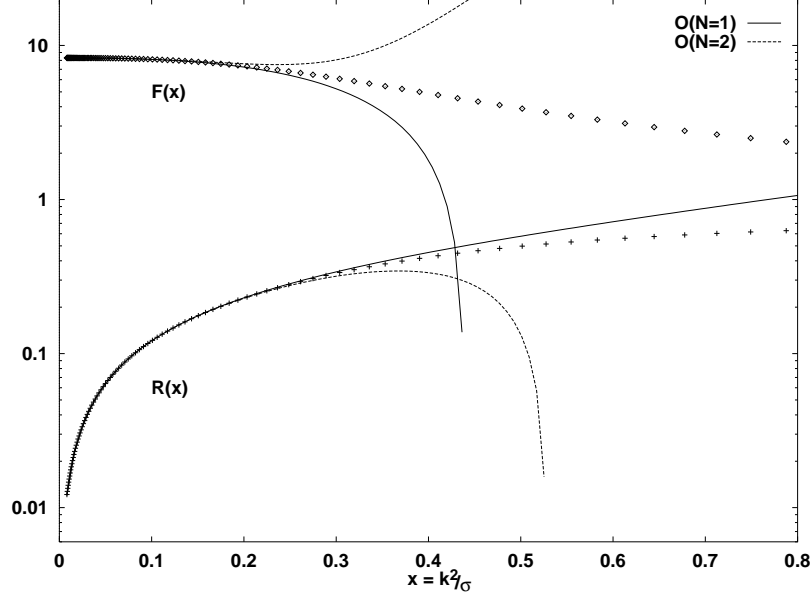


Figure 6: The numerical solutions of  $F(x)$  and  $R(x)$  for  $t = 0$  and  $b = 1$  together with their asymptotic expansions to order  $N = 1$  as well as  $N = 2$  at small  $x$ .

below). Furthermore, it can be verified numerically, that a solution for a value of  $b \neq 1$  for fixed  $t$  is identical to a solution for  $b = 1$  and  $t' = t b^{\nu/\kappa}$ , if  $x$  is substituted by  $x' = x/b^{1/\kappa}$ . This is the numerical manifestation of the scale invariance mentioned above (for  $\lambda = 1/b^{1/\kappa}$ ). Note that under scale transformations (107) the constant  $A$  trivially transforms according to its dimension,  $A \rightarrow A' = A/\lambda$ , without any adjustments from the way it is calculated, since

$$A' = A/\lambda = \lim_{x'_0 \rightarrow 0} \frac{7}{8} \left( \int_{x'_0}^{\infty} \frac{dy'}{y'^2} R(y') F^{2\delta}(y') - b' a^{2\delta} \frac{(x'_0)^{\kappa-1}}{1-\kappa} \right). \quad (108)$$

In figure 6 we plotted the numerically obtained solutions for  $F(x)$  and  $R(x)$  for  $b = 1$  and  $t = 0$  at small  $x$  together with their respective asymptotic forms to order  $N = 1$  and  $N = 2$ . The contributions of the order  $N = 2$  in the asymptotic expansion become comparable in size to the lower order at about  $x \simeq 0.2$  and dominant for increasingly higher values of  $x$ . The error in the asymptotic series being of the order of the first terms neglected, this is the usual indication for the range of  $x$  in which the asymptotic expansion to the given order can yield reliable results. In the particular calculation we used a value of about  $x_0 = 0.008$  for the matching point of the iterative process to the asymptotic result. This is obviously well below the estimated range of the validity of the asymptotic expansion.

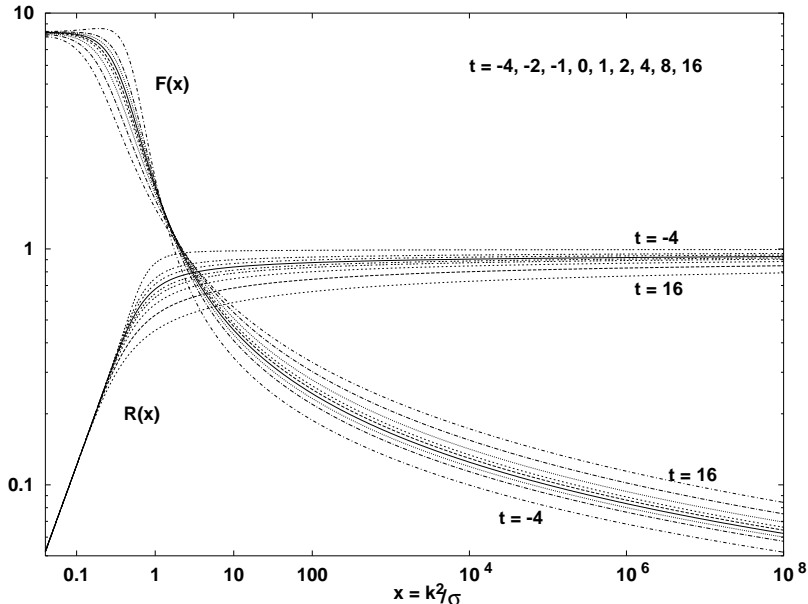


Figure 7: The numerical solutions of  $F(x)$  and  $R(x)$  with  $b = 1$  for different values of the parameter  $t = \{-4, -2, -1, 0, 1, 2, 4, 8, 16\}$  (solid lines represent  $t = 0$  solutions).

## 8 Numerical Results and Perturbative Limit

The numerical results were obtained with the order  $N = 1$  in the asymptotic expansion for which no dependence on  $x_0$  was observed for  $x_0 < 0.1$ . Higher values for the matching point are possible at higher orders. This shows that the expansion to next to leading order in the infrared ( $N = 1$ ) is sufficient to find numerically stable results for a satisfactory regime of matching points. Similar results follow for  $t \neq 0$ . We calculated  $F$  and  $R$  for several values in the range  $-5 \leq t \leq 16$ . At lower negative values the procedure became numerically unstable due to a developing (tachyonic) pole in  $F(x)$ . The fact that the integral equations for  $R$  and  $F$  possess a one-parameter family of solutions characterized by  $t$  is in fact the reason for the necessity of the infrared expansion up to next to leading order, since no stable solution can be found numerically without fixing the leading  $x$ -dependence of  $F(x)$  at small  $x$  by fixing the parameter  $t$ . This is a boundary condition to be imposed on the solutions from physical arguments.

In figure 7 the numerical results are plotted for different values of the parameter  $t$  (all with  $b = 1$ ). Perturbatively, we expect  $R(x)$  to approach a constant value and  $F(x) \rightarrow 1/\ln(\lambda x)$  for  $x \rightarrow \infty$ . The reason we introduced the constant  $\lambda$  in the one-loop running coupling  $F$  is that we fixed the momentum scale in our calculations by arbitrarily setting  $b = 1$ . The relation between the scale of perturbative QCD  $\Lambda_{\text{QCD}}$  and  $\sigma$  cannot be determined this way. Therefore, we set  $\Lambda_{\text{QCD}}^2 = \sigma/\lambda$  for some scale parameter  $\lambda$ . Qualitatively, all solutions display a similar behavior at



high momenta. The solutions for positive values of  $t$  seem to have more residual momentum dependence in  $R$  at high momenta than those for  $t \leq 0$ . A very good fit to the perturbative form can be obtained for  $t = -4.2$ . For negative values of  $t$ , however, the running coupling,  $\alpha_S(\mu) = F(s)/(4\pi\beta_0)$ , has a maximum,  $\alpha_{\max} > \alpha_c$ , at a finite value of the renormalization scale  $s = \mu^2/\sigma$ . This is because the dominant subleading term of the running coupling in the infrared is determined by  $t$ ,

$$F(x) \rightarrow a(1 - tx^\nu + D_{001}x^{3\kappa} + D_{100}x^{1+2\kappa}), \quad x \rightarrow 0. \quad (109)$$

With  $\nu \simeq 2.05 < 3\kappa < 1 + 2\kappa$  and  $D_{001} < 0$ , it is clear that for  $t < 0$  the running coupling increases for smallest scales close to  $\mu = 0$  before higher order terms dominate. There necessarily has to be a maximum  $\alpha_{\max} > \alpha_c$  at some finite scale  $\mu$  for any solution with  $t < 0$ . Such a maximum at finite scale implies a zero of the beta function which cannot be interpreted as a fixed point (since it appears at a finite scale  $\mu_0$ ). It is easy to see that the slope of the beta function  $\beta(g)$  at such a point  $g_{\max}$  is infinite. This precludes its possible classification as being infrared or ultraviolet stable. The present case ( $t < 0$ ) corresponds to a double valued  $\beta(g)$  with a positive branch and a negative branch coexisting for  $g_c < g < g_{\max}$ . In lack of an understanding of this scenario, we therefore disregard solutions for  $t < 0$  as likely to be unphysical.

In contrast, for  $t \geq 0$ ,  $\alpha_c = \alpha(\mu = 0)$  is the only maximum of the running coupling for all real values of the renormalization scale, and  $\alpha_c$  is thus a true infrared stable fixed point. Comparing the behavior of the resulting gluon and ghost renormalization functions in the ultraviolet we observe that, for the  $t \geq 0$  solutions, the case  $t = 0$  yields the best resemblance of their one-loop anomalous dimensions. We therefore restrict the discussion of our results to the case  $t = 0$  from now on, interpreting the existence of solutions for  $t \neq 0$  as a mathematical peculiarity.

In order to obtain an estimate of the factor  $\lambda$  to relate the infrared scale  $\sigma$  to the perturbative QCD scale  $\Lambda_{\text{QCD}}$ , we compare the results for the renormalization functions  $Z(x)$  and  $G(x)$  (with  $x = k^2/\sigma$ ) to their respective one-loop forms,

$$Z_{\text{pt}} = \left( \frac{\ln(\mu^2/\Lambda_{\text{QCD}}^2)}{\ln(k^2/\Lambda_{\text{QCD}}^2)} \right)^{1-2\delta} = \left( \frac{\ln(\lambda s)}{\ln(\lambda x)} \right)^{1-2\delta}, \quad \text{and} \quad (110)$$

$$G_{\text{pt}} = \left( \frac{\ln(\mu^2/\Lambda_{\text{QCD}}^2)}{\ln(k^2/\Lambda_{\text{QCD}}^2)} \right)^\delta = \left( \frac{\ln(\lambda s)}{\ln(\lambda x)} \right)^\delta. \quad (111)$$

In figure 8 we plot the functions  $Z(x)$  and  $G(x)$  as obtained from  $F(x)$  and  $R(x)$  (for  $t = 0$ ) according to the parameterization (70) along with their respective one-loop forms using  $\lambda = 1.8$ . The renormalization point  $s = \mu^2/\sigma = 1.18 \cdot 10^7$  (with  $Z(s) = G(s) = 1$ ) was chosen to be the numerical ultraviolet cutoff of the particular calculation for aesthetic reasons. A different choice would result in no more than a constant vertical shift of the curves on the logarithmic plot, and the choice of the renormalization point is thus absolutely inessential for the present consideration. It is possible to match one of the renormalization functions  $Z$  and  $G$  with its perturbative form even closer than in this figure by varying the value of  $\lambda$  in the perturbative

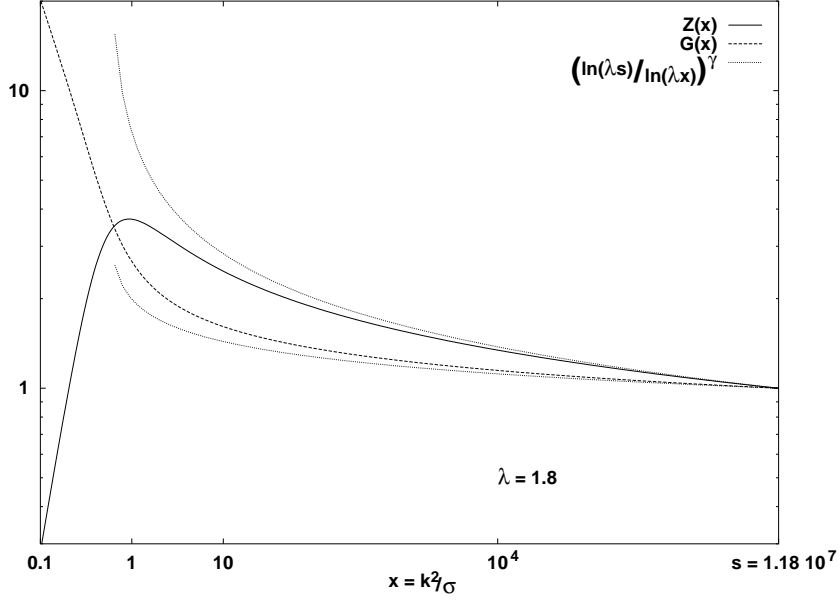


Figure 8: The renormalization functions  $Z(x)$  and  $G(x)$  obtained for  $t = 0$  and their leading logarithmic forms (with  $\gamma \rightarrow 1 - 2\delta$  for the gluon, and  $\gamma \rightarrow \delta$  for the ghost).

logarithms. This will, however, at the same time affect the perturbative form of the other renormalization function in the opposite direction, *e.g.*, for  $\lambda$  approximately  $4 \sim 5$  the perturbative logarithm of the gluon is hardly distinguishable from  $Z(x)$  for  $x > 10$  on the scales as used in figure 8, while a similarly good fit of the one-loop form to  $G(x)$  is obtained for  $0.2 \sim 0.3$ . To fit the perturbative logarithms at high momenta as close as possible to both renormalization functions with a unique value of  $\lambda$ , we can restrict its value approximately to the range  $1.5 \leq \lambda \leq 2$ .

For a scale factor in the same range,  $1.5 \leq \lambda \leq 2$ , the resemblance of the leading logarithms at high momenta can be optimized by an *unphysical* choice of the parameter  $t$  of approximately  $t = -4.2$ . The according solutions approach their leading logarithmic behavior at momenta as low as  $k^2 \simeq 10\sigma$  and are practically identical to the latter for all momenta higher than that. In contrast, as mentioned above, increasing positive values of  $t$  lead to solutions fit by the leading perturbative logarithms decreasingly well (see figure 9).

To summarize the discussion of our results at high momenta, we conclude that we obtain quite good agreement with the leading logarithmic behavior (as known from perturbation theory) for the renormalization functions  $Z$  and  $G$  at high momenta. The perturbative QCD scale parameter  $\Lambda_{\text{QCD}}$  is thereby related to the infrared scale  $\sigma$  by  $\Lambda_{\text{QCD}}^2 = \sigma/\lambda$ . The factor  $\lambda$  can be numerically estimated to be approximately  $1.5 - 2$ .

Note that even though we introduced a numerical ultraviolet cutoff, for sufficiently high values, our solutions to the ultraviolet finite equations for  $F(x)$  and  $R(x)$  show

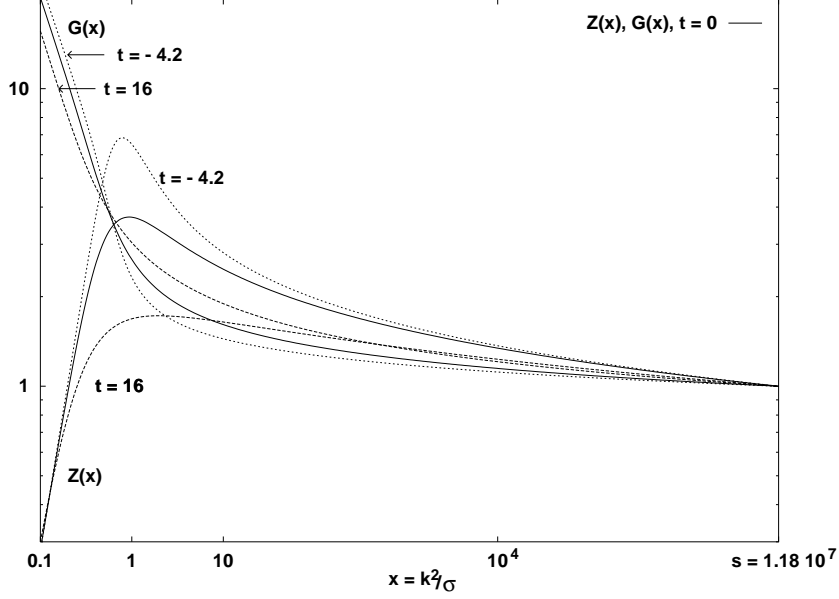


Figure 9: The renormalization functions  $Z(x)$  and  $G(x)$  for  $t = \{-4.2, 0, 16\}$ . Their leading logarithmic form at large  $x$  is not given (see fig. 8), it is indistinguishable from the  $t = -4.2$  results for  $x > 10$  (and with  $\lambda$  in  $1.5 - 2$ ).

no dependence on this cutoff. There are no ultraviolet boundary conditions imposed on the solutions. Fixing the infrared boundary condition by choosing a value for the parameter  $t$  (and the scale by setting  $b = 1$ ) we have no further influence on the high momentum behavior of the solutions which selfconsistently results from the iterative process alone. Deviations from leading logarithmic behavior can have several origins:

- Even though the gluon and ghost renormalization functions obey one-loop scaling, the non-perturbative running coupling,  $\alpha_S(\mu) = F(s)/(4\pi\beta_0)$ , contains two- and higher loop contributions (if certainly not all of them). Therefore, the fact that the results for  $t = 0$  approach the leading logarithmic behavior at higher momenta than some of the apparently unphysical results for negative values of  $t$  is not unreasonable.
- Depending on  $t$  also, the function  $R(x)$  can have residual momentum dependence even at very high momenta. In figure 7 the solution for, *e.g.*,  $t = -4$  approaches the value one at momenta as low as  $k^2 \simeq 10\sigma$ , whereas for positive  $t$  considerable logarithmic momentum dependence can be left even at  $k^2 \simeq 10^8\sigma$  (see fig 7 for  $t = 16$ ). While this has of course no influence on the running coupling, it does affect the asymptotic behavior of the renormalization functions.
- Since  $\ln(\lambda x) = \ln \lambda + \ln x$ , all different asymptotic forms used above yield an equivalent leading logarithmic contribution (in the limit  $x \rightarrow \infty$ ). The relevant

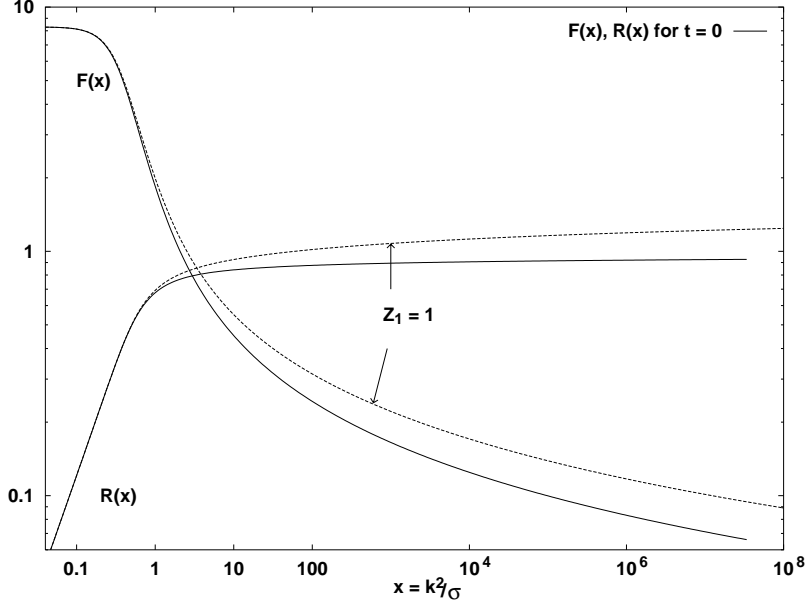


Figure 10: The functions  $F(x)$  and  $R(x)$  for  $t = 0$  compared to the respective results obtained from setting  $Z_1 = 1$ .

question is the one for the momentum scale above which the results should follow their leading logarithms in phenomenological applications.

Fixing the momentum scale in our calculations from the rough estimate  $\sigma = \lambda \Lambda_{\text{QCD}}^2$  given above is not satisfactory. Not only that the parameter  $\lambda$  is poorly determined, also the value of  $\Lambda_{\text{QCD}}$ , appropriate for the present subtraction scheme (and  $N_f = 0$ ), is not a phenomenologically well known quantity. We discuss in more detail in the next section, how to avoid this problem by fixing  $\sigma$  directly, independent of the precise values for  $\lambda$  and thus  $\Lambda_{\text{QCD}}$ . As a result of this, we find that  $k^2 \simeq 10\sigma$  corresponds to a momentum scale of 1GeV, and we conclude that the high momentum behavior of the solutions for  $t = 0$  is in reasonable agreement with the perturbative result.

In connection with the renormalization procedure discussed in the previous section we motivated the substitution of the cutoff dependence in the constant  $Z_1$  by a dependence on the integration momentum to improve the ultraviolet behavior of the solutions. In figure 10 we compare the  $t = 0$  results for  $F(x)$  and  $R(x)$  obtained this way (from eq. (85) for the running coupling  $F$ ) with those of an analogous calculation using (83) with  $Z_1 = c_{Z_1} = 1$  instead. It can be seen clearly that both solutions represent identical results in the infrared. This shows that the existence of the solutions and, in particular, of the infrared fixed point in the present truncation scheme is no artifact of the treatment we suggested for the renormalization constant of the 3-gluon loop  $Z_1$ . Furthermore, it verifies that this treatment does indeed

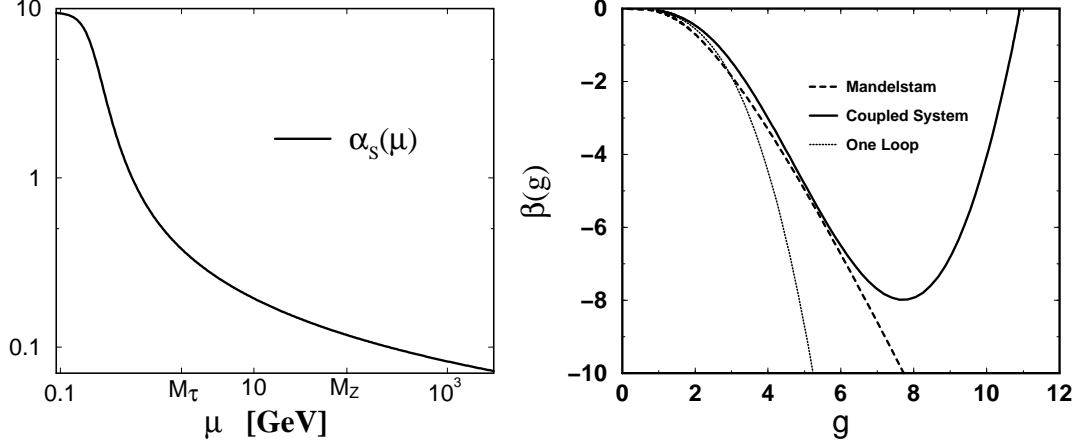


Figure 11: The running coupling  $\alpha_S(\mu)$  for  $t = 0$  (left), and the corresponding  $\beta$ -function (right) in comparison with its leading perturbative form (one-loop) and the  $\beta$ -function as a result of the Mandelstam approximation from ref. [9].

improve the ultraviolet behavior, noting that  $R(x)$  as obtained for  $Z_1 = 1$  does not approach a momentum independent constant in the ultraviolet on any reasonable scale.

## 9 Discussion of the Running Coupling

The running coupling of the present scheme is given in eq. (71) by

$$\alpha_S(\mu) = \frac{g^2(\mu)}{4\pi} = \frac{1}{4\pi\beta_0} F(s), \quad (112)$$

where  $s = \mu^2/\sigma$  involves the scale  $\sigma$  related to the infrared boundary condition  $b = 1$ . The result for  $\alpha_S(\mu)$  is shown in figure 11. To assign a value to the scale  $\sigma$  we use the phenomenological value of the running coupling  $\alpha_S(M_Z) = 0.118$  at the mass of the  $Z$ -boson,  $M_Z = 91.2$  GeV [50]. For the  $t = 0$  solution we obtain this way  $M_Z^2/\sigma \simeq 70000$  and therefore,  $\sigma \simeq (350\text{MeV})^2$ . From the comparison of the solutions for the renormalization functions  $Z$  and  $G$  to their leading logarithmic form at high momenta, this corresponds to a perturbative scale  $\Lambda_{\text{QCD}}$  in  $250 \sim 300$  MeV (for  $\lambda$  in  $1.5 \sim 2$ ). This is not a very significant result, however, since the value for  $\Lambda_{\text{QCD}}$  is dependent on the number of quarks  $N_f$  and the order of the perturbative expansion. In particular, in the present framework we expect it to change when quarks are included. The determination of the momentum scale in our scale invariant calculation from the dimensionless function  $F(s)$  (by  $\alpha_S(M_Z) \stackrel{!}{=} 0.118$ ) is independent of the value for the scale parameter  $\lambda$  and thus of the value for perturbative scale  $\Lambda_{\text{QCD}} = \sqrt{\sigma/\lambda}$ . Equally independent of this value is the ratio of the  $Z$ - to the  $\tau$ -mass,  $M_Z/M_\tau \simeq 51.5$ , and we obtain from this ratio the value  $\alpha_S(M_\tau) = 0.38$  for

the running coupling at the mass of the  $\tau$ -lepton. Even though this is in compelling agreement with the experimental value [50], we deliberately do not want to claim it to be a theoretical prediction. We regard this result as nothing but a consistency check of the present calculation which happens to yield better numbers than the present level of truncations and approximations might suggest.

The right panel of figure 11 shows the corresponding  $\beta$ -function with its two fixed points in the ultraviolet at  $g = 0$  and in the infrared at  $g = g_c \simeq 10.9$ . For comparison we plotted the leading perturbative form for  $g \rightarrow 0$  (and  $N_f = 0$ ),  $\beta(g) \rightarrow -\beta_0 g^3 = -11/(16\pi^2) g^3$ , and the infrared singular non-perturbative result obtained from the analogous subtraction scheme in the Mandelstam approximation according to ref. [9]. The solution to the coupled system of gluon and ghost Dyson-Schwinger equations yields better agreement with the leading perturbative form at small  $g$ , since due to neglecting ghosts, the leading coefficient was obtained to be  $\beta_0 = 14/(16\pi^2)$  in Mandelstam approximation [9]. While this can be regarded as small quantitative discrepancy, the significant difference between the present result and the Mandelstam approximation for  $g \geq 7$  once more demonstrates the importance of ghosts in Landau gauge, in particular, in the infrared.

## 10 A Comparison to Lattice Results

It is interesting to compare our solutions to lattice results available for the gluon propagator [34, 35] and for the ghost propagator [51] using lattice versions to implement the Landau gauge condition supplemented by different procedures to eliminate Gribov copies (at least approximately). Recently, for the pure  $SU(2)$  lattice gauge theory, the influence of such copies of gauge equivalent configurations present in the conventional Landau gauge, has been systematically investigated for gluons and ghosts in [52].

In figure 12 we compare our solution for the gluon propagator to the data from ref. [35]. The momentum scale in our results, fixed from  $\alpha_S(M_Z)$ , is not used as a free parameter. In order to account for the units used in ref. [35], we plotted the gluon propagator, normalized according to  $Z(x=1) \approx 11.3$ , as a function of the momentum  $x = k^2 a^2$  in units of the inverse lattice spacing, using  $a^{-1} = 2$  GeV corresponding to the value  $\beta = 6.0$  for  $SU(3)$  used in [35]. According to the authors of [35], the arrow indicates a bound below which finite size effects become considerable. As can be seen in figure 12, the essential features of our solution are beyond the scope of present lattice calculations. Due to different normalizations, lattice sizes and values of the lattice coupling  $\beta$ , it is not quite obvious that presently available lattice data for the gluon propagator in Landau gauge from the different groups [34] and [35] is indeed consistent. Since we prefer to adjust the units of our calculations rather than those of the lattice data, we apologize for choosing a particular set of data (from figure 3 in ref. [35]) and refer the reader to the literature, in order to assess the consistency of the different lattice results.

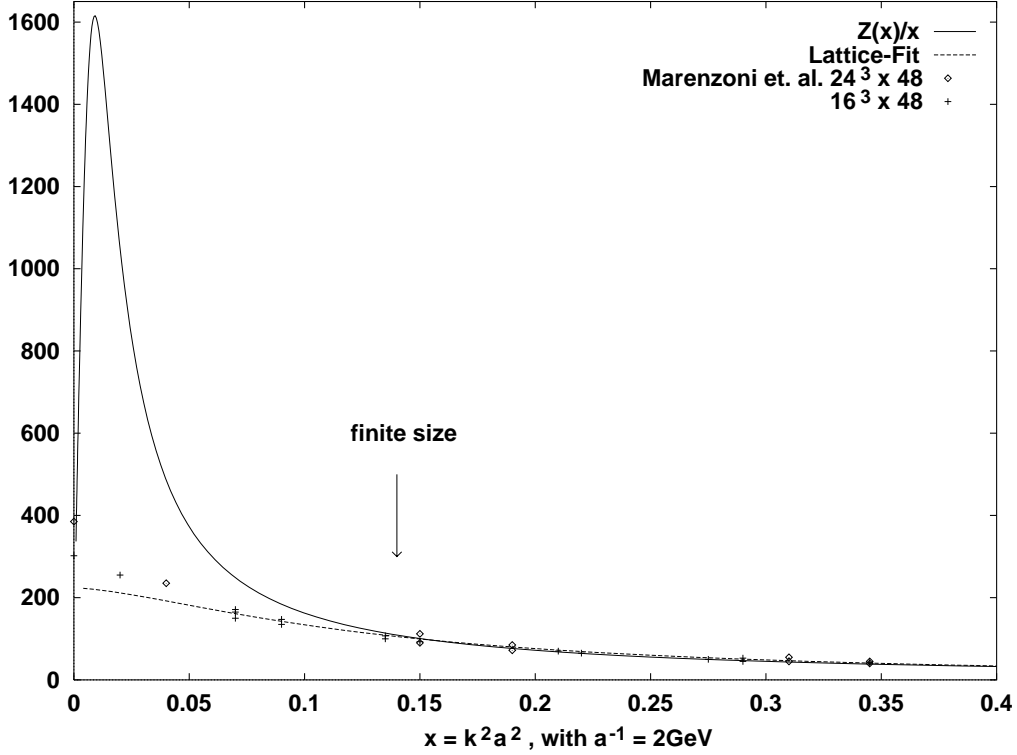


Figure 12: The numerical result for the gluon propagator from Dyson–Schwinger equations (solid line) compared to lattice data from fig. 3 in [35].

In figure 13 we compared our infrared enhanced ghost propagator with normalization such that  $G(x = 1) = 1$  to the results of ref. [51]. We choose to display the lattice results for the symmetric  $24^4$  and the non-symmetric  $16^3 \times 32$  lattices for  $SU(3)$  at  $\beta = 6.0$  from figure 1 in ref. [51] up to  $x \approx 3$ . Identical results modulo finite size effects were obtained for an  $8^4$  lattice (see ref. [51]). Again,  $x = k^2 a^2$  with  $a^{-1} = 2$  GeV and the momentum scale in our results, fixed from the  $Z$ -mass as described in the last section, is *not* adjusted.

The data extracted from the long direction of the  $16^3 \times 32$  lattice might indicate the existence of a finite maximum in the ghost propagator at very low momenta. The fact that the two lowest data points in this case lie significantly below their neighbors of the  $24^4$  lattice was interpreted by the authors of ref. [51] as a genuine signal rather than a finite size effect. The reason for this being that, on the  $8^4$  lattice, an enhancement due to finite size was observed for the lowest point in contrast to the shift downwards of the two points from the 32 direction of the non-symmetric lattice. No such maximum was observed on any of the smaller lattices. Our results do not confirm the existence of such a maximum in the ghost propagator but coincide

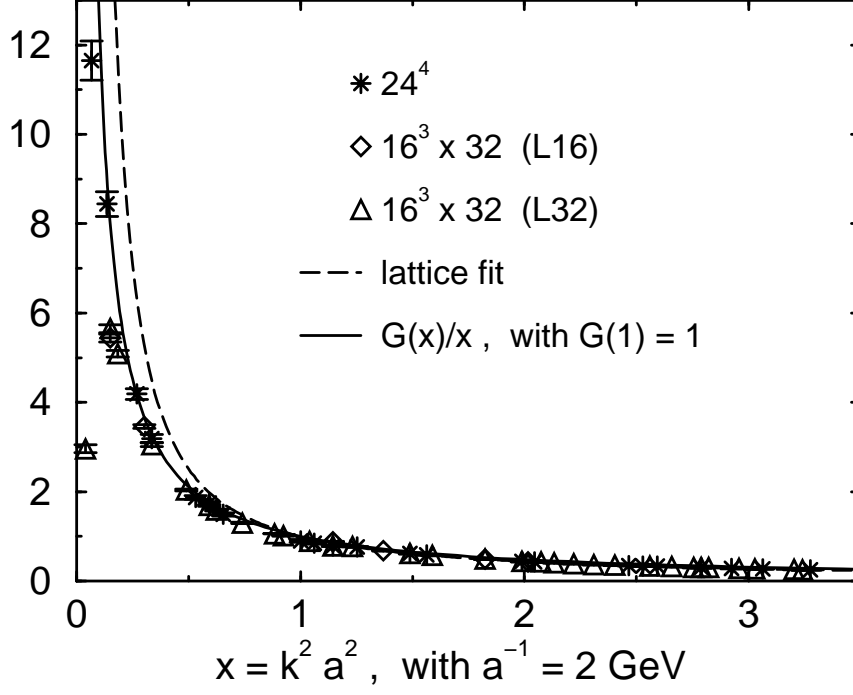


Figure 13: The numerical result for the ghost propagator from Dyson–Schwinger equations (solid line) compared to data from fig. 1 in ref. [51] for  $24^4$  and  $16^3 \times 32$  lattices, and a fit of the form  $c/x + d/x^2$  (with  $c = 0.744$ ,  $d = 0.256$ ) as obtained in ref. [51] for  $x \geq 2$  (dashed line).

nicely with all those data points of the differently sized lattices that lie on a universal curve. In addition, the  $24^4$  and  $16^3 \times 32$  lattices are of roughly the same size as the unsymmetric  $16^3 \times 48$  and  $24^3 \times 48$  lattices used for the gluon propagator in ref. [35]. Considering their investigation of finite size effects due to deviations between different components of the gluon propagator at small momenta, one might be led to question the significance of the maximum in the ghost propagator observed for one particular set of data in ref. [51] at momenta too low to yield finite size independent results for the gluon propagator, *c.f.*, ref. [35] on even larger lattices.<sup>1</sup>

It is quite amazing to observe that our numerical solution fits the lattice data at low momenta ( $x \leq 1$ ) significantly better than the fit to an infrared singular form with integer exponents,  $D_G(k^2) = c/k^2 + d/k^4$ , as given in ref. [51]. Clearly, low momenta ( $x < 2$ ) were not included in this fit, but the authors conclude that no reasonable fit of such a form is possible if the lower momentum data is to be

<sup>1</sup>Note the different  $x$ -ranges used in figures 12 and 13 and the position of the arrow indicating finite size effects to become considerable.



included. Therefore, apart from the question about a possible maximum at the very lowest momenta, the lattice calculation seems to confirm the existence of an infrared enhanced ghost propagator of the form  $D_G \sim 1/(k^2)^{1+\kappa}$  with non-integer exponent  $0 < \kappa < 1$ . The same qualitative conclusion has in fact been obtained in a more recent lattice calculation of the ghost propagator in  $SU(2)$  [52], where its infrared dominant part was fitted best by  $D_G \sim 1/(k^2)^{1+\kappa}$  for an exponent  $\kappa$  of roughly 0.3 (for  $\beta = 2.7$ ). This also is in qualitative agreement with the  $SU(2)$  calculations of ref. [51], again, with the exception of one data point for the lowest possible lattice momentum.

Furthermore, in refs. [51, 52] the Landau gauge condition was supplemented by algorithms to select gauge field configurations from the fundamental modular region which is to eliminate systematic errors that might occur due to the presence of Gribov copies.<sup>2</sup> Thus, the good agreement of our result with the lattice calculations suggests that the existence of such copies of gauge configurations might have little effect on the solutions to Landau gauge Dyson–Schwinger equations. This could also explain the similarity of our solutions to the qualitative behavior obtained by Zwanziger for gluon and ghost propagators from implications of complete gauge fixings [36].

## 11 Confined Gluons

Since we calculated Euclidean Green’s functions, or Schwinger functions, for gluon and ghost correlations, we resort to the Osterwalder–Schrader reconstruction theorem which states that a Gårding–Wightman relativistic quantum field theory can be constructed from a set of Schwinger functions if those Euclidean correlation functions obey certain conditions, the Osterwalder–Schrader axioms [53]. In particular, the axiom of *reflection positivity* for Euclidean Green’s functions is a direct result of the positive definiteness of the norm in the Hilbert space of the corresponding Gårding–Wightman quantum field theory. This condition involves arbitrary partial sums of  $n$ -point functions and is hardly provable in its general form. The special case of a single propagator  $G(x - y)$  reads, *i.e.*, the lowest partial sum,

$$\int d^4x d^4y \bar{f}(-x_0, \mathbf{x}) G(x - y) f(y_0, \mathbf{y}) \geq 0 \quad (113)$$

where  $f \in \mathcal{S}_+(\mathbb{R}^4)$  is a complex valued test (Schwartz) function with support in  $\{(x_0, \mathbf{x}) : x_0 > 0\}$ . This special case of reflection positivity can be shown to be a necessary and sufficient condition for the existence of a Lehmann representation of the Wightman distribution (the Minkowski space propagator) corresponding to  $G(x - y)$  [54]. Therefore, the construction of a counter example to this condition (by a suitable choice of  $f$ ) is sufficient to prove that the Euclidean correlation function cannot represent physical particle correlations which can be interpreted as a manifestation of confinement.

---

<sup>2</sup>An investigation of the effectiveness of the stochastic overrelaxation method to achieve this is given in ref. [52]

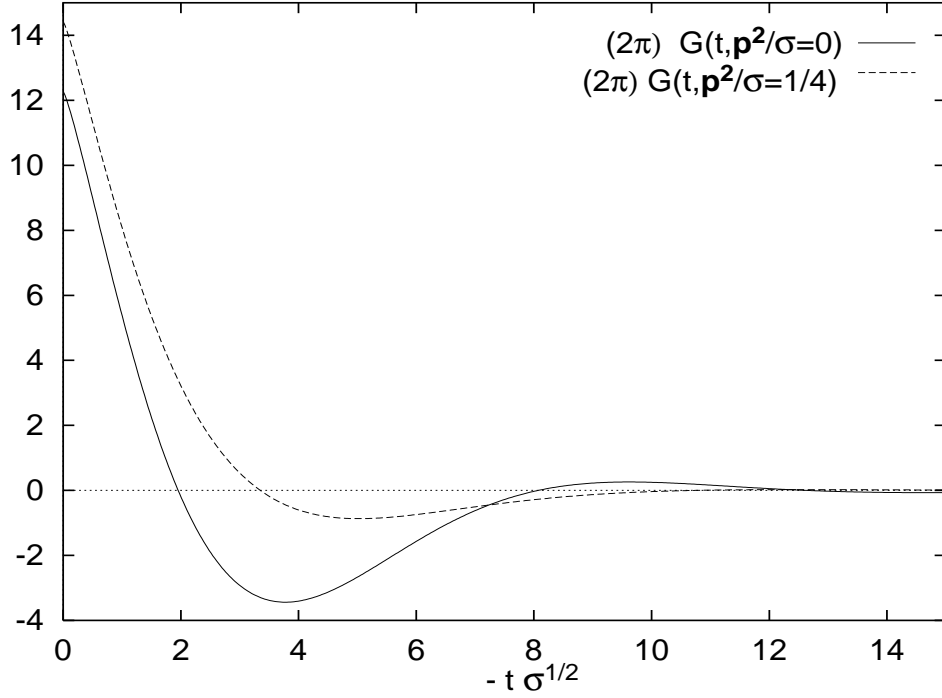


Figure 14: The one-dimensional Fourier transform of the gluon propagator,  $G(t, \mathbf{p}^2)$ .

Heuristically, we can rewrite the condition (113) after three dimensional Fourier transformation as

$$\int_0^\infty dt' dt \bar{f}(t') G(-(t' + t), \mathbf{p}) f(t) \geq 0, \quad (114)$$

where  $G(x_0, \mathbf{p}) := \int d^3x G(x_0, \mathbf{x}) e^{i\mathbf{p}\mathbf{x}}$ , and a separated momentum dependence of the analogous Fourier transform of the test function  $f$  has to provide for a suitable smearing around the three-momentum  $\mathbf{p}$ .

In figure 14 we plotted this Fourier transform of essentially the trace of the gluon propagator,

$$G(t, \mathbf{p}^2) := \int \frac{dp_0}{2\pi} \frac{Z(p_0^2 + \mathbf{p}^2)}{p_0^2 + \mathbf{p}^2} e^{ip_0 t}, \quad (115)$$

for  $\mathbf{p}^2 = 0$  and  $\mathbf{p}^2 = \sigma/4$ . Choosing a sufficiently small  $\mathbf{p}$  and a real function  $f(t)$  which peaks strongly around a point  $t_0/2$  for which  $G(-t_0, \mathbf{p}^2) < 0$ , it is now very easy to construct a counter example to condition (113) for the gluon propagator. We interpret this result as confined gluon correlations described by the Euclidean Green's function  $D_{\mu\nu}$ . The ghost propagator in Euclidean momentum space, being negative for positive renormalization functions  $G(k^2) > 0$  which is the case at tree-level already, trivially violates reflection positivity. This is of course due to the wrong spin-statistic of the ghost fields.

Note that the existence of zeros in the Fourier transform (115) for sufficiently small  $\mathbf{p}^2$  implies that the gluon propagator in coordinate space cannot have a well defined inverse for all  $(t, \mathbf{x})$ . While the corresponding singularities in  $G^{-1}(t, \mathbf{x})$  will cause problems in a Hubbard–Stratonovich transformation to bosonize effective non-local quark theories as the Global Color Model, see ref. [15], the same comment we gave at the end of section 4 applies here again. The infrared structure of the vertex functions, renormalization group invariance and the existence of zeros in the gluon propagator alone, all lead to the same conclusion: The combination of ghosts and gluons,  $g^2 G^2(k^2)Z(k^2)/k^2 = \alpha_S(k^2)/k^2$  is the physically important quantity that determines the interactions of quarks in Landau gauge (and the current–current interaction of the Global Color Model). We have verified explicitly that the Fourier transform of  $\alpha_S(k^2)/k^2$  is free of such zeros and positive.

## 12 Summary and Conclusions

We presented a selfconsistent solution for the propagators of gluons and ghosts within the Dyson–Schwinger equation approach to QCD in Landau gauge without quarks. A direct comparison of this solution to the gluon propagator from the Mandelstam approximation to its Dyson–Schwinger equation shows the tremendous importance of non-perturbative ghost contributions which are neglected in the Mandelstam approximation.

We introduced a systematic truncation scheme to close the infinite tower of Dyson–Schwinger equations at the level of 3-point vertex functions. This was possible by constructing these vertex functions from their respective Slavnov–Taylor identities. Such constructions, when contributions from irreducible 4-point scattering kernels are neglected in the Slavnov–Taylor identities, allow to express all 3-point vertex functions in terms of the scalar functions which parameterize the propagators of gluons, ghosts and quarks. This procedure is consistent with the truncation of the Dyson–Schwinger equations in which irreducible 4-point correlations are also neglected.

In this truncation scheme, at present without quarks, it is found that the leading infrared behavior of the gluon propagator is dominated completely by the ghost loop in the gluon DSE clearly demonstrating the importance of ghosts. In particular, an analytic discussion of the solutions to the closed set of equations for gluons and ghosts reveals that the infrared behavior of their 2-point functions is determined by an irrational exponent: The gluon propagator vanishes in the infrared as  $D(k) \sim (k^2)^{2\kappa-1}$ , and the ghost propagator is infrared enhanced (as compared to a free massless particle pole),  $D_G(k) \sim (1/k^2)^{\kappa+1}$ , where  $\kappa = (61 - \sqrt{1897})/19 \approx 0.92$ .

The non-perturbative definition of the running coupling  $\alpha_S(\mu^2)$  of our renormalization scheme is given by the renormalization group invariant product of the ghost and gluon renormalization functions  $G$  and  $Z$ , *i.e.*,  $4\pi\alpha_S(\mu^2) = g^2 G^2(\mu^2)Z(\mu^2)$ . Their infrared behavior implies the existence of an infrared stable fixed point at a

critical coupling,  $\alpha_c \simeq 9.5$ .

Both, the gluon and the ghost propagator compare favorably with recent results from lattice gauge simulations. Since these studies implemented various algorithms to avoid possible Gribov copies, in particular, those of the ghost propagator, the compelling agreement with our solution for the ghost propagator indicates that the Gribov problem might have little influence on the solutions to Dyson–Schwinger equations.

We have furthermore demonstrated that the gluon propagator obtained here violates Osterwalder–Schrader reflection positivity, and hence has no Lehmann representation, which we interpret as a signal for confinement. To study quarks and, most importantly, their confinement, the present framework will be extended to include the quark propagator selfconsistently in future.

We have given a variety of arguments in section 2 as to why our present results should not be sensitive to undetermined transverse terms in the 3–gluon vertex. However, the necessity of an additional assumption on the renormalization constant of the 3–gluon vertex to restore the ultraviolet behavior of the solutions, besides being due to neglecting 4–gluon correlations which appear at order  $g^4$ , might indicate that the possible presence of some additional purely transverse terms in the vertex should be taken into account also, in future.

The conclusions of the present work rely on the fact that there are no such undetermined transverse terms in the ghost–gluon vertex of the present truncation scheme. Therefore, in contrast to the ultraviolet (perturbative) behavior, the infrared behavior of the propagators, being entirely due to infrared dominant ghost contributions, is not affected by the details of the 3–gluon vertex. As for the gluon loop, we were able to proceed in close analogy to the Mandelstam approximation while accounting for ghost contributions. This allows a direct comparison and shows the influence of ghosts in Landau gauge clearly.

Nevertheless, the construction of transverse terms by means of constraints arising from multiplicative renormalizability in the case of the vertices in QCD will be an important future project. Such a construction, available at present for massless quenched QED [29], will be of particular importance when quarks are included in the selfconsistent framework.

It will be furthermore important to compare our present results to calculations which do not rely on a one–dimensional approximation for the integrals. In order to overcome this approximation, it will be necessary to extend the technique of asymptotic infrared expansions to the original equations including their full angular dependence. This analytic technique, developed and applied to the Mandelstam approximation previously [7, 9] and extended to the coupled system of gluon and ghost Dyson–Schwinger equations in the present paper, proved to be a necessary prerequisite to finding numerically stable solutions.

Since confinement might be realized by a quite different mechanism in a different gauge, and in order to assess the possibility of gauge artifacts in our results, it will be important to study different gauges in parallel. Such a study of a coupled system

of equations, analogous to the present one, which determines the gluon propagator in the ghost-free axial gauge while accounting for its complete tensor structure, is currently in progress [14].

## Acknowledgments

We thank F. Coester, F. Lenz, M. R. Pennington, H. Reinhardt and M. Schaden for helpful discussions. AH and RA gratefully acknowledge the hospitality of the Physics Division at Argonne during a visit in the early stages of this work. This work was supported by the DFG under contract Al 279/3-1, by the Graduiertenkolleg Tübingen (DFG Mu705/3), and the US Department of Energy, Nuclear Physics Division, contract number W-31-109-ENG-38.

We are indebted to A. Cucchieri for helping us become aware of a typo in Eqs. (83), (85) and (90) in previous versions of our manuscript.

## Appendix

### A The Identity for the Ghost–Gluon Vertex

Without irreducible ghost–ghost correlations, *c.f.*, eq. (14), the Slavnov–Taylor identity (13) decomposes into the irreducible ghost–gluon vertex function,  $G_\mu^{abc}(x, y, z)$ , and gluon and ghost propagators as follows,

$$\begin{aligned} \frac{1}{\xi} \int d^4u d^4v d^4w \partial_\mu^x D_{\mu\nu}(x-u) G_\nu^{acb}(u, v, w) D_G(z-v) D_G(w-y) \\ - \frac{1}{\xi} \int d^4u d^4v d^4w \partial_\mu^y D_{\mu\nu}(y-u) G_\nu^{bca}(u, v, w) D_G(z-v) D_G(w-x) \\ = g f^{abc} D_G(z-x) D_G(z-y) . \end{aligned} \quad (116)$$

From the Slavnov–Taylor identity for the gluon propagator,

$$\partial_\mu^x D_{\mu\nu}(x-u) = \xi \int \frac{d^4k}{(2\pi)^4} \frac{ik^\nu}{k^2} e^{ik(x-u)} ,$$

and with the ghost propagator

$$D_G(x-y) = \int \frac{d^4q}{(2\pi)^4} D_G(q) e^{iq(x-y)}$$

we obtain after Fourier transformation,

$$\begin{aligned} \frac{ik_\rho G_\rho^{abc}(k, q, p)}{k^2} D_G(p) D_G(q) - \frac{ip_\rho G_\rho^{abc}(-p, q, -k)}{p^2} D_G(-k) D_G(q) \\ = g f^{abc} (2\pi)^4 \delta^4(k+q-p) D_G(-k) D_G(p) . \end{aligned} \quad (117)$$

Here,  $G_\mu^{abc}(k, q, p)$  denotes the ghost–gluon vertex in momentum space which corresponds to the conventions used in section 2 up to the total momentum conserving  $\delta$ –function,

$$\begin{aligned} G_\mu^{abc}(k, q, p) &= \int d^4x d^4y d^4z G_\mu^{abc}(x, y, z) e^{-ikx} e^{-iqy} e^{ipz} \\ &= (2\pi)^4 \delta^4(k + q - p) G_\mu^{abc}(p, q) . \end{aligned}$$

Using this in eq. (117) one obtains eq. (15) for the ghost–gluon vertex function.

## B 3–Gluon Vertex with Tree–Level Ghost Coupling

In this appendix we demonstrate that the Slavnov–Taylor identity for the 3–gluon vertex in presence of ghosts in Landau gauge has no solution assuming a tree–level form for the ghost–gluon coupling. Neglecting irreducible contributions from the ghost–gluon scattering kernel, *i.e.*, setting  $\tilde{G}_{\mu\nu}(p, q) = \delta_{\mu\nu}$ , the Slavnov–Taylor identity for the 3–gluon vertex function in Landau gauge simplifies to the following equation,

$$ik_\rho \Gamma_{\mu\nu\rho}(p, q, k) = G(k^2) \left\{ \mathcal{P}_{\mu\nu}(q) \frac{q^2}{Z(q^2)} - \mathcal{P}_{\mu\nu}(p) \frac{p^2}{Z(p^2)} \right\} . \quad (118)$$

Following the general Ansatz of ref. [26] for those parts of the 3–gluon vertex which can be constrained by its Slavnov–Taylor identity, we write,

$$\begin{aligned} \Gamma_{\mu\nu\rho}(p, q, k) &= -A(p^2, q^2; k^2) \delta_{\mu\nu} i(p - q)_\rho - B(p^2, q^2; k^2) \delta_{\mu\nu} i(p + q)_\rho \\ &\quad - C(p^2, q^2; k^2) (\delta_{\mu\nu} p q - p_\nu q_\mu) i(p - q)_\rho + \frac{1}{3} S(p^2, q^2, k^2) i(p_\rho q_\mu k_\nu + p_\nu q_\rho k_\mu) \\ &\quad + \text{cyclic permutations} . \end{aligned} \quad (119)$$

The most general tensor structure contains these 10 terms plus 4 purely transverse terms involving 2 more scalar functions [26]. The latter cannot be constrained by Slavnov–Taylor identities and are generally omitted. The scalar functions appearing in (119) have the following symmetry properties,

$$A(x, y; z) = A(y, x; z) , \quad B(x, y; z) = -B(y, x; z) , \quad C(x, y; z) = C(y, x; z) ,$$

and  $S(x, y, z)$  is totally antisymmetric with respect to any two arguments. With this Ansatz in (118) we obtain the following equations from comparing the coefficients of the independent tensors on both sides:

$$\begin{aligned} \delta_{\mu\nu} : \quad & \left( A(x, y; z) - B(x, y; z) \right) y - \left( A(x, y; z) + B(x, y; z) \right) x \\ &= \left( \frac{y}{Z(y)} - \frac{x}{Z(x)} \right) G(z) \end{aligned} \quad (120)$$

$$\text{and} \quad -2B(x, y; z) + C(x, y; z) (x - y) = 0 , \quad (121)$$

$$q_\mu q_\nu : \quad -2A(z, y; x) + A(x, z; y) - B(x, z; y) - \frac{1}{2}(z + x - y)S(x, y, z) = -\frac{G(z)}{Z(y)}, \quad (122)$$

$$p_\mu p_\nu : \quad \text{same as above for } q_\mu q_\nu \text{ with } x \leftrightarrow y ,$$

$$p_\mu q_\nu : \quad -A(z, y; x) - B(z, y; x) + A(x, z; y) - B(x, z; y) = 0 , \quad (123)$$

$$q_\mu p_\nu : \quad -2B(x, y; z) - 2A(z, y; x) + 2A(x, z; y) - zS(x, y, z) = 0 . \quad (124)$$

The first observation here is that with (124) in (123) we find that

$$S(x, y, z) = 0 . \quad (125)$$

We could than in principle use (124) to eliminate  $B$  in (122) thus obtaining an equation for  $A$ . Eq. (124) would then give us the corresponding function  $B$  which would fix  $C$  from (121). However, eliminating  $B$  from (122) yields,

$$A(x, y; z) - A(x, z; y) + A(z, y; x) = \frac{G(z)}{Z(y)} . \quad (126)$$

From the necessary symmetry of  $A(x, y; z)$  it follows that the l.h.s. in (126) is symmetric under exchange of  $x$  and  $z$  whereas the r.h.s. is not. It is therefore not possible to find a solution  $A$  for this equation with the correct symmetry.

This can be cured in two ways. The first is to allow for a non-trivial ghost-gluon scattering kernel of the form given in eq. (10) in section 2 which would not affect the ghost-gluon vertex since the correction to the kernel is transverse in the momentum of the incoming ghost. With the Ansatz (10) we can redo the above analysis obtaining modifications to the different terms on the r.h.s. of eqs. (120) to (122). In particular, eq. (120) is replaced by

$$\begin{aligned} & \left( A(x, y; z) - B(x, y; z) \right) y - \left( A(x, y; z) + B(x, y; z) \right) x \\ &= \left( \frac{y}{Z(y)} \left( 1 + y a(z, y; x) \right) - \frac{x}{Z(x)} \left( 1 + x a(z, x; y) \right) \right) G(z) , \end{aligned} \quad (127)$$

eq. (121) by,

$$-2B(x, y; z) + C(x, y; z) (x - y) = \left( \frac{y a(z, y; x)}{Z(y)} - \frac{x a(z, x; y)}{Z(x)} \right) G(z), \quad (128)$$

and eq. (129) by

$$-2A(z, y; x) + A(x, z; y) - B(x, z; y) = -\frac{G(z)}{Z(y)} \left( 1 + y a(z, y; x) \right) . \quad (129)$$

Eqs. (123) and (124) remain unchanged and, in particular,  $S = 0$ , which we used in (129) already. Defining

$$f(z, x; y) := \frac{G(z)}{Z(y)} \left( 1 + y a(z, y; x) \right) , \quad (130)$$

we realize that the program outlined above to obtain the functions  $A, B$  and  $C$  can give a solution if  $f(x, y; z) = f(y, x; z)$ . The equation to obtain  $A$  which replaces (126) is now,

$$A(x, y; z) - A(x, z; y) + A(z, y; x) = f(z, x; y) . \quad (131)$$

Note that using (124) here again, this yields,

$$A(x, y; z) - B(x, y; z) = f(z, x; y) , \quad (132)$$

showing that a solution to (131) for  $A$  with  $B$  obtained from (124) also satisfies (127). With  $C$  from (128) we find that all necessary equations (127,128,129) and (123,124) are solved (with  $S = 0$ ). So far, we did not specify the unknown function  $a(x, y; z)$  resulting from a non-trivial ghost-gluon scattering kernel. The necessary symmetry of  $f(x, y; z)$  provides certainly not enough information to fix  $a(x, y; z)$  completely. However, since we do not want to modify the scaling properties of the vertex artificially, it may seem reasonable to solve the system of equations with an Ansatz for  $f(x, y; z)$  as the most general sum of terms representing ratios  $G/Z$  with all possible arguments  $x, y$  and  $z$  obeying the necessary symmetry of  $f$  in its first two arguments. This restriction, which yields terms of the same structure as the r.h.s. of eq. (126) now in (131), allows to determine the function  $a(x, y; z)$  up to an unknown constant  $\Delta$ ,

$$\begin{aligned} a(x, y; z) = & \frac{1}{y} \left( \frac{G(z)}{G(x)} - \frac{G(y)}{G(x)} \right) - \frac{\Delta}{2y} \left\{ \frac{G(y)}{G(x)} \left( \frac{Z(y)}{Z(z)} + \frac{Z(y)}{Z(x)} - 2 \right) \right. \\ & \left. + \frac{G(z)}{G(x)} \left( 1 - \frac{Z(y)}{Z(x)} \right) + 1 - \frac{Z(y)}{Z(z)} \right\} . \end{aligned} \quad (133)$$

The solutions for  $A, B$  and  $C$  follow as outlined above, in this case,

$$\begin{aligned} A(x, y; z) = & \frac{1}{2} \left( \frac{G(z)}{Z(x)} + \frac{G(z)}{Z(y)} \right) + \frac{1 - \Delta}{2} \left( \frac{G(x)}{Z(y)} + \frac{G(y)}{Z(x)} \right) \\ & - \frac{1 - \Delta}{2} \left( \frac{G(x)}{Z(x)} + \frac{G(y)}{Z(y)} \right) , \end{aligned} \quad (134)$$

$$\begin{aligned} B(x, y; z) = & \frac{1}{2} \left( \frac{G(y)}{Z(x)} - \frac{G(x)}{Z(y)} \right) + \frac{1 - \Delta}{2} \left( \frac{G(z)}{Z(x)} - \frac{G(z)}{Z(y)} \right) \\ & - \frac{1 - \Delta}{2} \left( \frac{G(x)}{Z(x)} - \frac{G(y)}{Z(y)} \right) - \frac{\Delta}{2} \left( \frac{G(x)}{Z(z)} - \frac{G(y)}{Z(z)} \right) , \end{aligned} \quad (135)$$

$$C(x, y; z) = \frac{1}{x - y} \left( \frac{G(z)}{Z(x)} - \frac{G(z)}{Z(y)} \right) . \quad (136)$$

This solution to the 3-gluon Slavnov-Taylor identity corresponds to a specific form for the ghost-gluon scattering kernel, in the simplest case, for  $\Delta = 0$ , the dependence on ratios of gluon renormalization functions  $Z$  disappears and it is given by

$$\tilde{G}_{\mu\nu}(p, q) = \delta_{\mu\nu} + \frac{1}{q^2} \frac{G(k^2) - G(q^2)}{G(p^2)} (\delta_{\mu\nu} p q - p_\nu q_\mu) . \quad (137)$$



The second way to account for the presence of ghosts in the Slavnov–Taylor identity in Landau gauge is to consider a possible dressing of the ghost–gluon vertex function as described in section 2. For the present truncation scheme this led to a vertex as given in eq. (21) from the new Slavnov–Taylor identity (13). The structure of the corresponding ghost–gluon scattering kernel as far as it is relevant to the 3–gluon Slavnov–Taylor identity, however, is then simply

$$\tilde{G}_{\mu\nu}(p, q) = \frac{G(k^2)}{G(q^2)} \delta_{\mu\nu} , \quad (138)$$

which, used in the Slavnov–Taylor identity (9), led to eq. (24). The solution to this equation, as given in eqs. (25/26) in section 2, can be obtained from an entirely analogous procedure as outlined in this appendix, setting,

$$f(x, y; z) = \frac{G(x)G(y)}{G(z)Z(z)} , \quad (139)$$

as it corresponds to the *Abelian*–like identity (24). This results in the solution  $A(x, y; z) = A_+(x, y; z)$ ,  $B(x, y; z) = A_-(x, y; z)$  and  $C(x, y; z) = 2A_-(x, y; z)/(x - y)$  with the notations of section 2. The latter way to implement ghost contributions in the construction of the 3–gluon vertex function from its Slavnov–Taylor identity is considerably simpler than the alternative as described in this appendix (based on a tree–level ghost–gluon vertex), and it is furthermore much more consistent with the assumption underlying the truncation scheme of section 2.

## C Functions in the 3–Gluon Loop

Below we give the functions  $N_1$  and  $N_2$  which appear in the 3–gluon loop of the gluon DSE using the solution (25/26) for the 3–gluon vertex function and contracting the gluon DSE with the projector  $\mathcal{R}_{\mu\nu}(k)$  of eq. (47) (see sec. 4),

$$\begin{aligned} N_1(x, y; z) = & \frac{29x}{4} + \frac{x^2}{4y} + \frac{29y}{4} + \frac{y^2}{4x} + \frac{(9x^2 + 50xy + 9y^2)z}{4xy} \\ & - \frac{9(x+y)z^2}{4xy} - \frac{z^3}{4xy} + \frac{24x^2 - 10xy + y^2}{2(z-x)} + \frac{24y^2 - 10xy + x^2}{2(z-y)} \end{aligned} \quad (140)$$

and

$$\begin{aligned} N_2(x, y; z) = & \frac{5x^3 + 41x^2y + 5xy^2 - 3y^3}{4x(y-x)} + \frac{x^2 - 10xy + 24y^2}{2(y-z)} \\ & + \frac{x^3 + 9x^2y - 9xy^2 - y^3}{xz} + \frac{(2x^2 + 11xy - 3y^2)z}{2x(x-y)} + \frac{(x+y)z^2}{4x(y-x)} . \end{aligned} \quad (141)$$

## References

- [1] T. Kinoshita, J. Math. Phys. **3** (1962) 650;  
T. D. Lee and M. Nauenberg, Phys. Rev. **133**, 6B (1964) 1549.  
Also referred to as the *non-Abelian Bloch-Nordsieck conjecture*, *c.f.*,  
F. Bloch and A. Nordsieck, Phys. Rev. **52** (1937) 54.
- [2] W. Marciano and H. Pagels, Phys. Rep. **36** (1978) 137.
- [3] T. Kinoshita and A. Ukawa, Phys. Rev. D **13** (1976) 1573.  
For a discussion in terms of the coherent state approach, see  
C. A. Nelson, Nucl. Phys. **B186** (1981) 187.
- [4] E. C. Poggio and H. R. Quinn, Phys. Rev. D **14** (1976) 578.
- [5] D. J. Gross and A. Neveu, Phys. Rev. D **10** (1974) 3235.
- [6] S. Mandelstam, Phys. Rev. D **20** (1979), 3223.
- [7] D. Atkinson et. al. J. Math. Phys. **22** (1981), 2704;  
D. Atkinson, P. W. Johnson and K. Stam, J. Math. Phys. **23** (1982), 1917.
- [8] N. Brown and M. R. Pennington, Phys. Rev. D **39** (1989), 2723;  
N. Brown, Ph. D. Thesis, University of Durham, August 1988.
- [9] A. Hauck, L. v. Smekal und R. Alkofer, e-print, hep-ph/9604430,  
Comp. Phys. Comm., in press.
- [10] M. Baker, J. S. Ball and F. Zachariasen, Nucl. Phys. **B186** (1981), 531; 560;  
Nucl. Phys. **B226** (1983), 455.
- [11] W. J. Schoenmaker, Nucl. Phys. **B194** (1982), 535.
- [12] J. R. Cudell and D. A. Ross, Nucl. Phys. **B358** (1991), 247.
- [13] K. Büttner and M. R. Pennington, Phys. Rev. D **52** (1995), 5220.
- [14] R. Alkofer, M. R. Pennington, L. v. Smekal and P. Watson, work in progress.
- [15] P. C. Tandy, Prog. Part. Nucl. Phys. **39** (1997), 11.
- [16] C. D. Roberts and A. G. Williams, Prog. Part. Nucl. Phys. **33** (1994), 477.
- [17] V. A. Miranski, “Dynamical Symmetry Breaking in Quantum Field Theories”,  
World Scientific, 1993, and references therein.
- [18] R. Delbourgo and M. D. Scadron, J. Phys. G **5** (1979), 1621.
- [19] H. J. Munczek and P. Jain, Phys. Rev. D. **46** (1992), 438.
- [20] R. T. Cahill, Austr. J. Phys. **42** (1989), 171.
- [21] N. Ishii, W. Bentz and K. Yazaki, Nucl. Phys. **A 587** (1995), 617.
- [22] G. Hellstern et al., Nucl. Phys. **A627** (1997), 67.
- [23] L. v. Smekal, A. Hauck and R. Alkofer, Phys. Rev. Lett. **79** (1997), 3591.

- [24] L. G. Vachnadze, N. A. Kiknadze and A. A. Khelashvili, Theor. Math. Phys. **102** (1995), 34.
- [25] U. Bar-Gadda, Nucl. Phys. **163** (1980), 312.
- [26] J. S. Ball and T.-W. Chiu, Phys. Rev. D **22** (1980), 2550.
- [27] S. K. Kim and M. Baker, Nucl. Phys. **B164** (1980), 152.
- [28] J. C. Taylor, Nucl. Phys. **B33** (1971), 436.
- [29] N. Brown and N. Dorey, Mod. Phys. Lett. **A6** (1991), 317;  
D. C. Curtis and M. Pennington, Phys. Rev. D **42** (1990), 4165
- [30] U. Ellwanger, M. Hirsch and A. Weber, Eur. Phys. J. **C1** (1998), 563.
- [31] N. Brown and M. R. Pennington, Phys. Rev. D **38** (1988), 2266.
- [32] E. J. Eichten and F. L. Feinberg, Phys. Rev. D **10** (1974), 3254.
- [33] J. S. Ball and T.-W. Chiu, Phys. Rev. D **22** (1980), 2542.
- [34] C. Bernard, C. Parrinello and A. Soni, Phys. Rev. D **49** (1994), 1585; D. S. Henty, O. Oliveira, C. Parinello and S. Ryan, Phys. Rev. D **54** (1996), 6923.
- [35] P. Marenzoni, G. Martinelli, and N. Stella, Nucl. Phys. **B455** (1995), 339.
- [36] D. Zwanziger, Nucl. Phys. B **412** (1994), 657; Nucl. Phys. B **378** (1992), 525.
- [37] U. Häbel, R. Könnig, H.-G. Reusch, M. Stingl and S. Wigard, Z. Phys. A **336** (1990) 423; 435.
- [38] M. Stingl, Z. Phys. A **353** (1996) 423.
- [39] J. Ahlback, A. Streibl and M. Schaden, “Non-perturbative Solutions to the Dyson-Schwinger Equations of Pure QCD”, in the Proceedings of the Workshop on QCD Vacuum Structure, Paris, France, June 1-5, 1992, eds. B. Müller and H. Fried, World Scientific.
- [40] M. Stingl, talk given at the Workshop on Dyson–Schwinger Techniques in QCD, Erlangen, Germany, February 5, 1997.
- [41] L. G. Vachnadze, N. A. Kiknadze, K. Sh. Turashvili and A. A. Khelashvili, Theor. Math. Phys. **100** (1994), 811.
- [42] G. B. West, Phys. Lett. **B115** (1982), 468.
- [43] G. B. West, Phys. Rev. D **27** (1983), 1878.
- [44] See *Physical and Nonstandard Gauges*, proceedings, workshop, Vienna, Austria, Sept. 19-23, 1989, edited by P. Gaigg, W. Kummer and M. Schweda, Vienna Tech. U., Springer (1990) (Lecture notes in physics, 361).
- [45] H. Cheng and E.-C. Tsai, Phys. Rev. D **36** (1987), 3196; M. Lavelle and M. Schaden, Phys. Lett. **B217** (1989), 551.
- [46] F. Lenz, H. W. L. Naus, K. Otha and M. Thies, Ann. Phys. **233** (1994), 12; 51.  
F. Lenz, H. W. L. Naus and M. Thies, Ann. Phys. **233** (1994), 317.

- [47] T. Kugo, *The Universal Renormalization Factors  $Z_1/Z_3$  and Color Confinement Condition in Non-Abelian Gauge Theory*, Kyoto Univ. preprint, KUNS-1368, 1995, hep-th/9511033.
- [48] H. Hata, Prog. Theor. Phys. **67** (1982), 1607, and **69** (1983), 1524.
- [49] G. t'Hooft, Nucl. Phys. **B72** (1974), 461.
- [50] Particle Data Group, Phys. Rev. D **54** (1996), 77.
- [51] H. Suman and K. Schilling, Phys. Lett. **B373** (1996), 314.
- [52] A. Cucchieri, Nucl. Phys. **B508** (1997), 353.
- [53] See, *e.g.*, R. Fernández, J. Fröhlich and A. Sokal, *Random Walks, Critical Phenomena and Triviality in Quantum Field Theory*, and R. Haag, *Local Quantum Physics*, both Texts and Monographs in Physics, Springer (1992), and references therein.
- [54] We are indebted to F. Coester for pointing this out to us.